İSTANBUL TECHNICAL UNIVERSITY ★ INFORMATICS INSTITUTE

THE INTERACTIONS OF METAL IONS WITH THYMINE TAUTOMERS: A COMPUTATIONAL STUDY

M.Sc. Thesis by

Semra BAYAT

Department: Computational Science and Engineering

Programme: Computational Science and Engineering

Supervisor : Assist. Prof. Dr. F. Aylin KONUKLAR

JULY 2007

İSTANBUL TECHNICAL UNIVERSITY ★ INFORMATICS INSTITUTE

THE INTERACTIONS OF METAL IONS WITH THYMINE TAUTOMERS: A COMPUTATIONAL STUDY

M.Sc. Thesis by

Semra BAYAT

(702041012)

Date of submission : 7 May 2007

Date of defence examination: 13 June 2007

Supervisor (Chairman): Assist. Prof. Dr. F. Aylin KONUKLAR

Members of the Examining Committee Prof. Dr. Viktorya AVİYENTE (B.Ü.)

Prof. Dr. Mine YURTSEVER (İ.T.Ü.)

JULY 2007

İSTANBUL TEKNİK ÜNİVERSİTESİ ★ BİLİŞİM ENSTİTÜSÜ

TİMİN VE TOTOMERLERİNİN METAL İYONLARI İLE ETKİLEŞİMLERİNİN İNCELENMESİ: HESAPSAL BİR ÇALIŞMA

YÜKSEK LİSANS TEZİ

Semra BAYAT
(702041012)

Tezin Enstitüye Verildiği Tarih : 7 Mayıs 2007
Tezin Savunulduğu Tarih : 13 Haziran 2007

Tez Danışmanı : Yard. Doç. Dr. F. Aylin KONUKLAR
Diğer Jüri Üyeleri Prof. Dr. Viktorya AVİYENTE (B.Ü.)
Prof. Dr. Mine YURTSEVER (İ.T.Ü.)

TEMMUZ 2007

ACKNOWLEDGEMENT

I want to thank my supervisor Assistant Prof. Dr. Fethiye Aylin Konuklar for her guidance and patience through my studies in my master thesis. I would like to thank Assoc. Prof. Dr. Cenk Selçuki for his suggestions and guidance.
I owe my best thanks to all my colleagues in the CSE department for their helpful relationships and psychological support.
Computer facilities support for this study was received from High Performance Computing Center, Institute of Informatics. I wish to acknowledge State Planning Organization and Tubitak 105E067 project for the financial support.

I want to dedicate this thesis to my lovely family.

July, 2007 Semra Bayat

TABLE OF CONTENTS

LIST OF ABBREVIATIONS

DNA : Deoxyribonucleic acid
HF : Hartree-Fock
DFT : Density Functional Theory
B3LYP : Becke 3-Parameter Lee-Yang-Parr Functional
LYP : Lee-Yang-Parr
LDA : Local Density Approximation
SCF : Self Consistent Field
ZPE : Zero Point Energy
BSSE : Basis Set Superposition Error
APT : Atomic Polar Tensor
T : Thymine
M : Metal
NBO : Natural Bond Orbital

LIST OF TABLES

LIST OF FIGURES

LIST OF SYMBOLS

N	**:** Number of electron
V	**:** Potential field
E	**:** Energy of the particle
$\mathbf{E^J}$	**:** Electron-electron repulsion term
$\mathbf{E^T}$	**:** Kinetic energy term
$\mathbf{E^V}$	**:** Potential energy term
$\mathbf{E^{XC}}$	**:** Exchange-correlation term
$\mathbf{E^C (\rho)}$	**:** Correlation functionals
$\mathbf{E^X (\rho)}$	**:** Exchange functionals
h	**:** Planck's constant
$\mathbf{\hat{H}}$	**:** Hamiltonian operator
m	**:** Mass
ΔE	**:** Relative energy
IE	**:** Interaction energy
$\mathbf{E_{BSSE}}$	**:** BSSE corrected energy
$\mathbf{\Delta E_{BSSE}}$	**:** BSSE corrected relative energy

TİMİN VE TOTOMERLERİNİN METAL İYONLARI İLE ETKİLEŞİMLERİNİN İNCELENMESİ: HESAPSAL BİR ÇALIŞMA

ÖZET

Nükleik asitlerin yapı ve fonksiyonları büyük ölçüde metal iyonlardan etkilenir. Katyonlar DNA bazları ve çift sarmalın stabilize edilmesinde görev alır. Metal iyonlarının nükleobazın yanında bulunması, bazdaki elektron dağılımını ve de totomerik dengeyi büyük ölçüde etkilemektedir. Başka bir deyişle, metal iyonları seyrek bulunan totomerlerin varolmasını sağlarken, bu totomerlerin varlığı ise nokta mutasyonu dahil çeşitli biyokimyasal süreçlerin oluşumunu sağlar. Bu çalışmanın hedefi Li^{+}, Na^{+}, K^{+}, Be^{+2}, Mg^{+2}, Ca^{+2}, Cu^{+}, Cu^{+2} ve Fe^{+2} metalleri ile timin, timin totomerleri ve metillenmiş timin türevlerinin etkileşimini açıklamaktır.

Çalışmada 8 farklı timin keto/enol totomeri ve onların metillenmiş türevleri modellenmiştir. Metal iyonları ile timin ve tüm totomerilerinin etkileşimlerini araştırmak için gaz fazında çalışılmıştır. Bunun için hesaplar Yoğunluk Fonksiyonel Teorisi (YFT) ile B3LYP/6-31++G** seviyesinde Gaussian 03 program paketi kullanılarak yapılmıştır.

Metal katyonları ve timin totomerleri arasında katyon-π and katyon-heteroatom bağlanmaları bulunmuştur. Bir katyon, timin molekülünde birden fazla bağlanma noktası olmasından dolayı aynı timin yapısı ile birden fazla katyon-heteroatom kompleksi oluşturabilmektedir. Totomer kararlılıklarının aynı grup elementleri için azalan atom numarası ile azaldığı görülmüştür. Totomer kararlılık sırasının N1-metillenmesi ile etkilenmediği ama metal etkileşiminden önemli ölçüde etkilendiği görülmüştür.

THE INTERACTIONS OF METAL IONS WITH THYMINE TAUTOMERS: A COMPUTATIONAL STUDY

SUMMARY

The structure and the function of the nucleic acids are in general depending on metal ions. Cations play an important role in stabilizing as well as destabilizing the DNA bases and the double helix. The presence of metal ions near bases can strongly affect the electron distribution in the bases and thus also the tautomeric equlibria. In other words, the effect of the metal ions can favor the formation of the rare tautomers, which are believed to be involved in various biochemical processes including point mutation. The aim of the study is to elucidate the interactions of Li^{+}, Na^{+}, K^{+}, Be^{+2}, Mg^{+2}, Ca^{+2}, Cu^{+}, Cu^{+2} and Fe^{+2} with all possible tautomers of thymine and its methylated derivatives.

In this study, eight optimized structure of keto/enol tautomers of thymine and its methylated derivatives are modeled. All tautomers are taken into account to investigate the effects of metal ion-thymine interactions in the gas phase. For this purpose, density functional theory (DFT) has been used at B3LYP/6-31++G** level by using Gaussian 03 program package.

Both cation-π and cation-heteroatom binding were observed between metal cations and thymine tautomers. The same cation could form more than one cation-heteroatom complex with the same structure due to more than one possible binding site in a nucleobase. It was observed that stabilities of tautomers decreases with increasing atomic number for the same group elements and the order of stability is not affected by methylation from N1 site but significantly affected by metalation.

1. INTRODUCTION

Chemistry of nucleic acid had started with studies of F. Miescher in the late 1860s. He came up with the isolation of the nucleic acid from human pus cells [1]. During the 1920s, biochemist P.A. Levene analyzed the components of the DNA molecule. He found that four nitrogenous bases were present: cytosine, thymine, adenine, and guanine; deoxyribose sugar; and a phosphate group (Figure 1.1). He concluded that the basic unit (nucleotide) was composed of a base attached to a sugar and that the phosphate was also attached to the sugar. Since then, great efforts have been made in the field of nucleic acid chemistry [2]. In the early 50s, Watson and Crick observed the double helix structure of DNA, which is stabilized by hydrogen bonds between

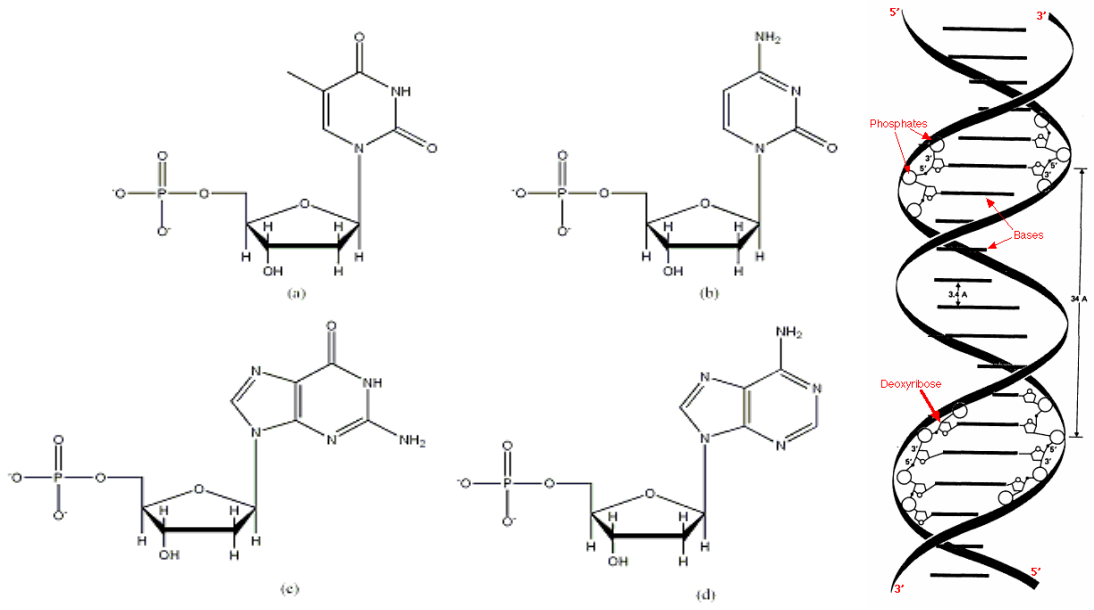

(I) (II)

Figure 1.1: Nucleotide Structures (I) (a) Thymine (b) Cytosine (c) Guanine (d) Adenine (II) double helix structure of DNA.

bases attached to the two strands and the sugars are joined together by phosphate groups that form phosphodiester bonds between the third and fifth carbon atoms of adjacent sugar rings. They showed that each strand of the DNA molecule was a

template for the other (Figure 1.1). During cell division the two strands separate and on each strand a new "other half" is built, just like the one before. This way DNA can reproduce itself without changing its structure - except for occasional errors, or mutations [3].

Nucleic acids function through their interactions with other molecules. Most thought interaction was Watson-Crick base pair, but researches showed that nucleobases could interact not only with each other but also with organic molecules and metals. Metal ions play an important role in several biological processes of nucleic acids such as synthesis, replication, structural integrity, and cleavage of DNA and RNA [4]. The interactions can influence the conformation and therefore the properties of DNA.

The main effect of metal binding is neutralizing the negatively charged backbone phosphate groups, but also modifying hydrogen bonds and stacking interactions can take place with the bases to stabilize the double helix [5]. It is known that tautomerism of nucleobases has an important role in DNA mutation [6]. The effect of the metal ions can favor the formation of the rare tautomers which are believed to be involved in various biochemical processes including point mutation [7-11]. The researches on the importance of nucleic acid-metal ions interactions traced back to 1900s. In 1924, Einar Hammarsten had stated that 'Na^+ and other available metal cations' would be required in the cell nucleus to balance the negative charge of (what was later called) DNA [12]. Ever since then the metal ion-nucleic acids studies have started. There are various experimental and computational metal-nucleic acid interaction studies in literature. These studies can be basically classified as metal ions interacting with nucleobases [13-22], metal ions interacting with phosphate groups of nucleotides [14] and metal ions interacting with base pairs [23-25].

Del Bene studied Li^+ affinity of DNA bases by ab initio calculations with the STO-3G basis sets [26]. Cerda and Wesdemiotis [4] have reported the alkali metal ions (Li^+, Na^+ and K^+) affinities of the DNA bases, but they do not show the information on the binding site of the metal. Burda et al. have studied on the interaction of guanine and adenine with various mono and bivalent metal cations at the Hartree-Fock (HF) and Moller-Plesset second-order perturbation theory (MP2); base pairs with various metal ions at HF and MP2 level [19,24]. Monajjemi et al studied alkali metals with thymine and tautomers by ab initio and DFT methods at HF and B3LYP

level [22]. However the results are not sufficient to predict the preferred location of the binding sites and the best conformers. They also do not present investigation on the interaction of the divalent metal cations with thymine and methylated thymine tautomers.

Many experimental studies have been carried out to shed a light on the structural aspects of metal–binding sites in DNA/RNA/proteins [27]. Cations at high concentration interact with nucleic acid bases and destroy the hydrogen bonding between base pairs but at low concentration cations may interact with negatively charged (electronegative) phosphate groups of nucleic acid to provide charge neutralization [4]. Presence of electronegative nitrogen and oxygen atoms as lone pairs, the nucleobases can act as metal ligands. Single nucleobases can interact with metal ions at any site including the carbon atoms but some sites are more preferable than the others. Spectroscopic and X-ray data shows that the N7 atom of the purine or N3 of pyrimidine residues, exocyclic O atoms, the phosphate oxygen atoms are the preferential sites of metal binding [28].

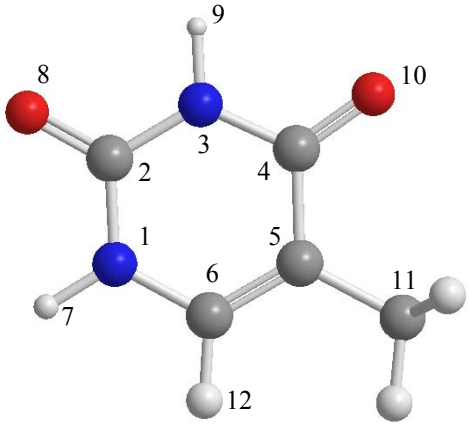

Figure 1.2: Common form of thymine nucleobase with numbering.

Nucleic acids are polymers which are composed of nucleotides. Each nucleotide consists of heterocyclic ring, phosphate group and pentose sugar. The heterocyclic rings are, in general, the purine and the pyrimidine bases. Thymine is one of the pyrimidine nucleobases. It is also known as 5-methyluracil, because it may be derived by methylation of uracil at the 5th carbon. Systematic name of thymine is 5-Methylpyrimidine-2,4(1*H*,3*H*)-dione ($C_5H_6N_2O_2$, 2-oksi-4-oksi-5-metilpirimidin, 2,4-dioksi-5-metilpirimidin, 5-metilurasil). Thymine (**T**) is found in the DNA and binds to adenine (A) via two hydrogen bonds to assist in stabilizing the nucleic acid

structures. In RNA, thymine is replaced with uracil. The structure and numbering systems for canonical thymine are given in Figure 1.2.

The thymine molecule may exist in various tautomeric forms differing from each other by the position of the protons, which may be bound to either ring nitrogen atoms or oxygen atoms. The five different keto-enol tautomers and three possible N1-methylated derivatives are given in Figure 1.3.

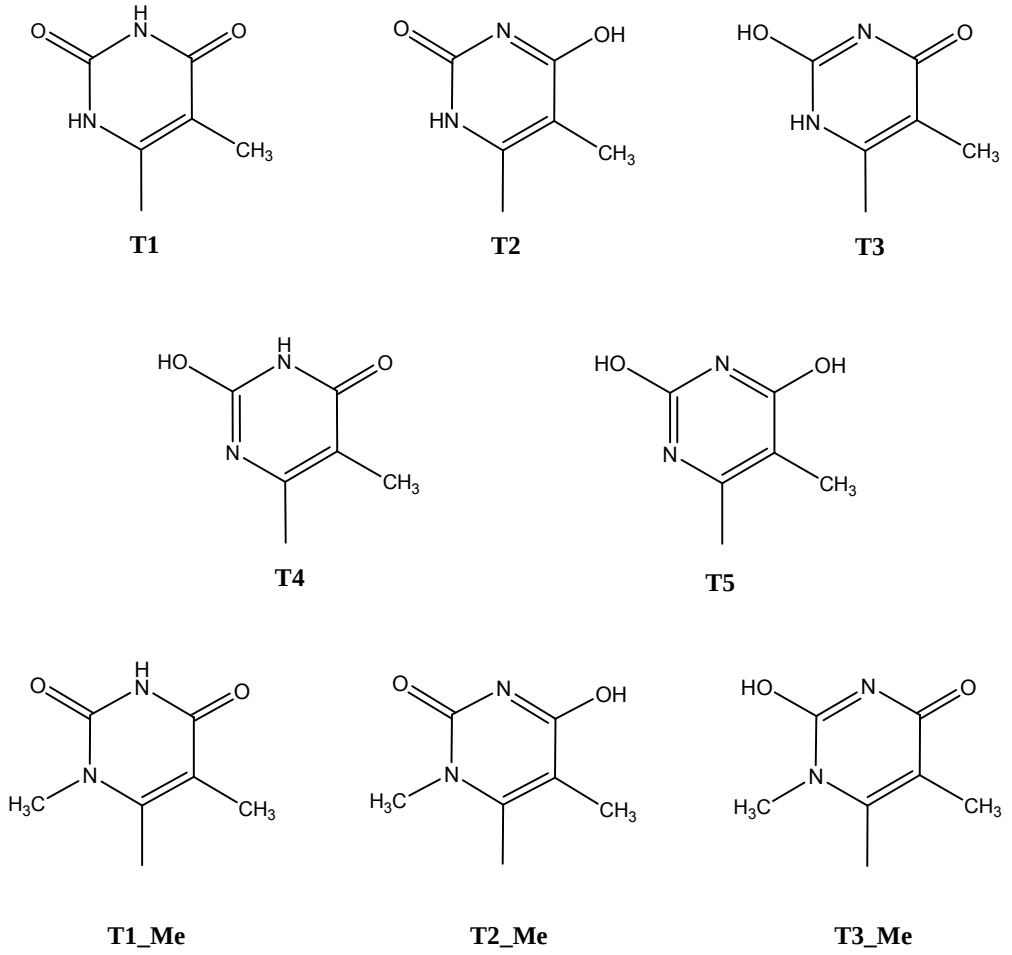

Figure 1.3: Structures of all tautomers of thymine and N1-methylated derivatives.

In the literature, the presence of metal ions Na^{+}, K^{+}, Mg^{+2} and Ca^{+2} in cells as neurotransmitters is pointed out. And several diseases may be related to metal ion depletion and some are related to the exceeding of optimal concentrations levels. On the other hand, the toxicity of heavy metal ions may depend partly on their binding to specific DNA sites [28].

To understand the role of cations in DNA, it is necessary to carry out a detailed interaction study of cations with all tautomers and conformers of bases. Although

there are number of studies related to metal-thymine interaction in the literature, the interactions of metals with all tautomers and its methylated derivates were not investigated yet. This study is an extension of theoretical studies of thymine, which aimed to investigate the effects of monovalent (Li^{+}, Na^{+}, K^{+}, Cu^{+}) and divalent (Be^{+2}, Mg^{+2}, Ca^{+2}, Cu^{+2} and Fe^{+2}) metal cations on the thymine base. The results will enable us to figure out more reliable conclusions for nucleobase-metal ion interactions. For this purpose, density functional theory (DFT) has been used at B3LYP/6-31++G** level by using the Gaussian 03 program package [29].

2. METHODOLOGY

We are perhaps not far removed from the time when we shall be able to submit the bulk of chemical phenomena to calculation.

Joseph Louis Gay-Lussac.(1888)

The binding of metal ions to nucleic acids has been subject of study for many years. To understand the structure and dynamic of DNA, many experimental and computational techniques, e.g. high-resolution X-ray crystallography, NMR spectroscopy and molecular dynamics simulations have been performed. Over the last three decades the methods of quantum chemistry have shown an impressive development: a large number of reliable and efficient approximations to the solution of the non-relativistic Schrödinger and the relativistic Dirac equation, respectively, are available. Currently quantum chemical methods are on the edge of being applied to realistic problems [30]. The uses of quantum chemical methods in observing the electronic and structural properties of DNA have high computational cost. The rapid development of computer hardware and software in the last three decade, led to a broad application of quantum chemistry methods to the study of the structure and stability of the nucleic acids base pairs [31].

2.1 Theory

2.1.1 Density Functional Theory

The Density Functional Theory (DFT) approach is based upon a strategy of modeling electron correlation via general functionals of the electron density

$$E = E[\rho(r)] \tag{2.1}$$

The Hamiltonian operator (H) in Schrödinger Equation $H\psi = E\psi$ depends only on the positions and atomic numbers of the nuclei and the total number of electrons. Such a dependence on total number of electrons suggests that it would be sufficient to find a physical observable to simplify construction of the operator. This would be

electron density ρ, which is integrated over all space, gives the number of electrons (N) of the system.

$$N = \int \rho(r) dr \qquad \textbf{(2.2)}$$

The first approximate model based on this idea was developed in the late 1920's by Thomas and Fermi [32]. Their approach was replacing the problem of calculating N-electron wave function by that of calculating the electron density in three-dimensional position space. Their results were not accurate enough because of the absence of the interaction between electrons, but this density-based functional suggested a new direction to solve many-body problem. This approach contains some of the basic concepts of what has since become DFT. In 1964, Pierre Hohenberg and Walter Kohn [33] proved that for molecules with a non-degenerate ground-state, the ground-state molecular energy, wave function, and all other molecular electronic properties are uniquely determined by the ground-state electronic probability density. The Hohenberg-Kohn theorem only proved that there exists a density functional, but did not give the details of the form of that functional. In 1965, Kohn and Sham [34] proposed a self-consistent procedure to apply DFT to atomic and solid-state calculations. Following the work of Kohn and Sham, the approximate functionals employed by current DFT methods partition the electronic energy into several terms

$$\mathrm{E} = \mathrm{E}^{\mathrm{T}} + \mathrm{E}^{\mathrm{V}} + \mathrm{E}^{\mathrm{J}} + \mathrm{E}^{\mathrm{XC}} \qquad \textbf{(2.3)}$$

where E^{T} is the kinetic energy term (arising from the motion of the electrons), E^{V} includes terms describing the potential energy of the nuclear-electron attraction and of the repulsion between pairs of nuclei, E^{J} is the electron-electron repulsion term (it is also described as the Coulomb self-interaction of the electron density), and E^{XC} is the exchange-correlation term and includes the remaining part of the electron-electron interactions.

All terms except the nuclear-nuclear repulsion are functions of ρ, the electron density. EJ is given by the following expression

$$E^{J} = \frac{1}{2} \int\int \rho(r_1)(\Delta r_{12})^{-1} \rho(r_2) dr_1 dr_2 \qquad \textbf{(2.4)}$$

Hohenberg and Kohn demonstrated that E^{XC} is determined entirely by the electron density. In practice, E^{XC} is usually approximated as an integral involving only the spin densities and possibly their gradients

$$E^{XC}(\rho) = \int f(\rho_\alpha(r), \rho_\beta(r), \nabla\rho_\alpha(r), \nabla\rho_\beta(r)) d^3r \quad \textbf{(2.5)}$$

The ρ_α refer to the α spin density, ρ_β refer to the β spin density, and ρ refer to the total electron density ($\rho_\alpha + \rho_\beta$).

E^{XC} is usually divided into separate parts, referred to as the exchange and correlation parts, but actually corresponding to the same-spin and mixed-spin interactions,

$$E^{XC}(\rho) = E^{X}(\rho) + E^{C}(\rho) \quad \textbf{(2.6)}$$

The two components on the right side of equation 2.6 are termed exchange functionals and correlation functionals. Both components can be of two distinct types: local functionals depend on the electron density ρ only, while gradient – corrected functionals depend on both ρ and its gradient∇ρ.

The local exchange functional is virtually always defined as follows:

$$E^{X}_{LDA} = -\frac{3}{2}\left(\frac{3}{4\pi}\right)^{1/3} \int \rho^{4/3} d^3r \quad \textbf{(2.7)}$$

where ρ is a function r. This form was developed to reproduce the exchange energy of a uniform electron gas. By itself, however, it has weakness in describing molecular systems.

Becke formulated the following gradient-corrected exchange functional [35] based on the LDA exchange functional in 1988, which is now in wide use:

$$E^{X}_{Becke88} = E^{X}_{LDA} - \gamma \int \frac{\rho^{4/3} x^2}{(1 + 6\gamma \sinh^{-1} x)} d^3r \quad \textbf{(2.8)}$$

where $x = \rho^{-4/3} |\nabla\rho|$. γ is a parameter chosen to fit the known exchange energies of the inert gas atoms, and Becke defines its value as 0.0042 Hartrees. As equation 2.8 makes clear, Becke's functional is defined as a correction to the local LDA exchange functional, and it succeeds in remedying many of the LDA functionals deficiencies.

In the Kohn-Sham DFT calculations, the equations need to be solved in a self-consistent way in an iterative manner. Under a specific approximation (like LDA),

the form of the equation is fixed. Then the iteration procedure is applied as it is shown in the flow chart (Figure 2.1).

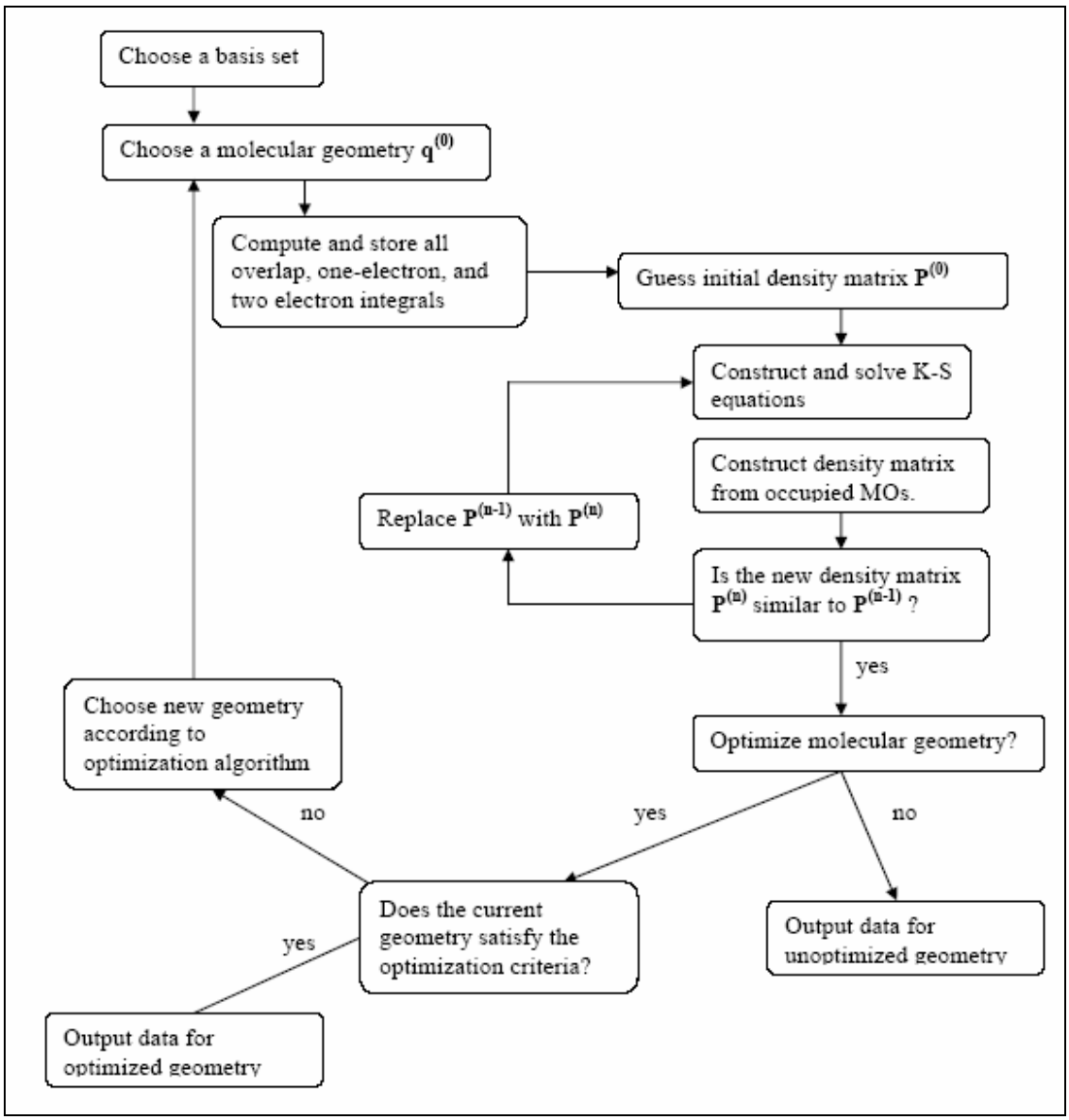

Figure 2.1: Flow chart of the KS-SCF procedure

Pure DFT methods are defined by pairing an exchange functional with a correlation functional. For example, the well-known BLYP functional pairs Becke's gradient-corrected exchange functional with the gradient-corrected correlation functional of Lee, Yang and Parr [36].

2.1.2 Hybrid Functionals

Hartree-Fock theory also includes an exchange term as part of its formulation. Recently, Becke has formulated functionals which include a mixture of Hartree-Fock and DFT exchange along with DFT correlation, conceptually defining E^{XC} as:

$$E_{hybrid}^{XC} = c_{HF}E_{HF}^{x} + c_{DFT}E_{DFT}^{XC} \quad \textbf{(2.9)}$$

where the c's are constants.

The correlation functional used in this study is the Lee-Yang-Parr (LYP) correlation functional. The closed shell LYP functional is given by:

$$E_c = -a\int \frac{1}{1+d\rho^{-1/3}}\left\{\rho + b\rho^{-2/3}\left[C_F\rho^{5/3} - 2t_w + (\frac{1}{9}t_w + \frac{1}{18}\nabla^2\rho)\right]e^{-c\rho^{-1/3}}\right\}dr \quad \textbf{(2.10)}$$

where

$$t_w = \frac{1}{8}\frac{|\nabla\rho(r)|^2}{\rho(r)} - \frac{1}{8}\nabla^2\rho \quad \textbf{(2.11)}$$

and a=0.04918, b=0.132, c=0.2533 and d=0.349. Hybrid functionals have proven to be superior to the traditional functionals.

2.1.3 Basis Sets

The basis functions are usually centered on the atomic nuclei and so bear some resemblance to atomic orbitals. An individual molecular orbital is defined as:

$$\phi_i = \sum_{\mu=1}^{N} c_{\mu p}x_\mu \quad \textbf{(2.12)}$$

where the coefficients $c_{\mu i}$ are known as the molecular orbital expansion coefficients. The basis functions $x_1 \ldots\ldots x_N$ are also chosen to be normalized. x_μ refers to an arbitrary basis function in the same way that ϕ refers to an arbitrary molecular orbital.

Ab initio electronic structure programs use Gaussian-type atomic functions as basis functions. Linear combinations of primitive gaussians are used to form the actual basis functions; the latter are called contracted Gaussians and have the form:

$$x_\mu = \sum_p d_{\mu p}g_p \quad \textbf{(2.13)}$$

where the $d_{\mu p}$ `s are fixed constants within a given basis set.

All of these constructions result in the following expansion for molecular orbitals:

$$\phi_i = \sum_{\mu} c_{\mu i} x_{\mu} = \sum_{\mu} c_{\mu i} \left(\sum_{p} d_{\mu p} g_p \right) \qquad \textbf{(2.14)}$$

2.2 Computational Details

2.2.1 Systems

In search of the global minimum, several initial geometries of thymine were considered. The five possible tautomers and three methylated tautomers were examined and their geometries were fully optimized after a detailed conformational search. The presences of these tautomers were confirmed by harmonic vibrational frequency calculations. The systems used in the calculations consist of deoxyribose

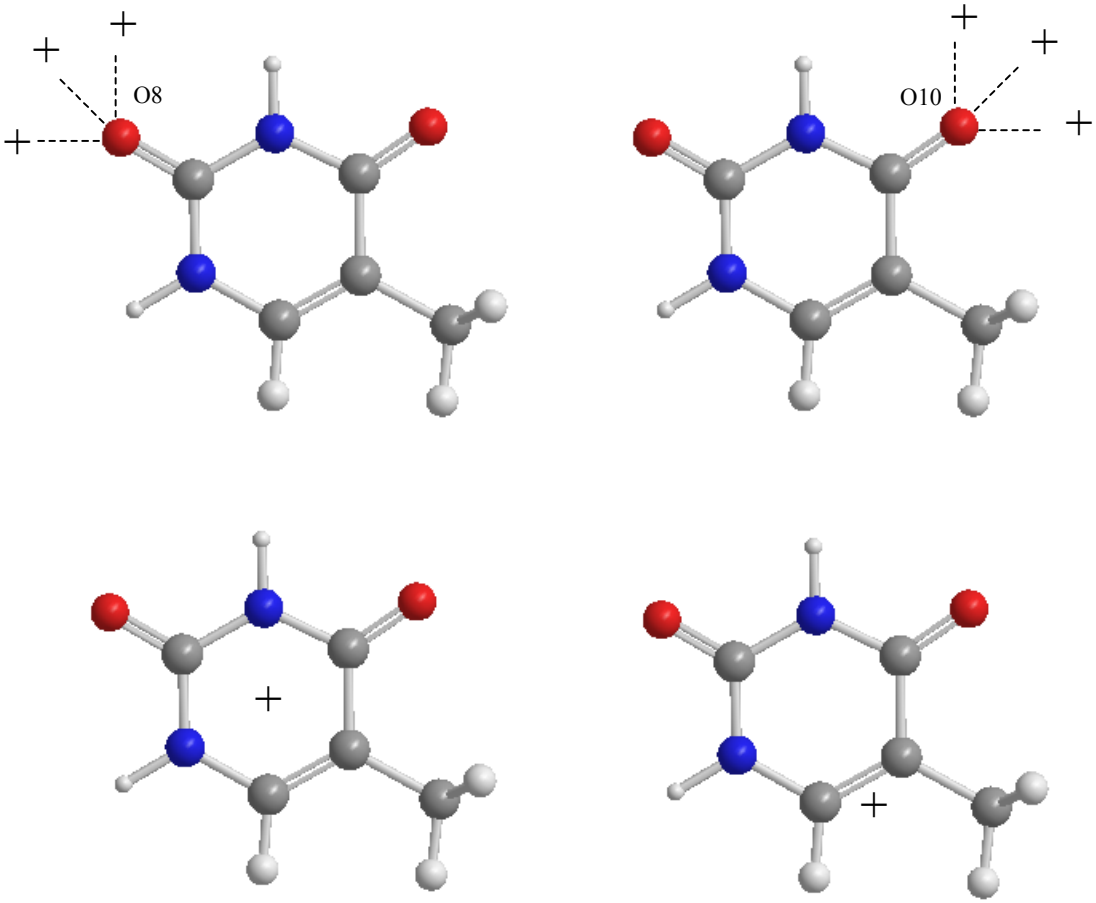

Figure 2.2: Initial positions of metal cations in complexes.

nucleobase thymine complexed with IA, IIA group elements (Li^+, Na^+, K^+, Be^{+2}, Mg^{+2}, Ca^{+2}) and transition metals (Cu^+, Cu^{+2}, Fe^{+2}). The cations were placed at the near heteroatoms (N1, N3, O8, O10) of the base lying in the same plane (cation-heteroatom complex) and located above the nucleobase ring interacting with all ring atoms of the nucleobase (cation-π complex) (Figure 2.2). Gas phase is chosen to see the binding energies, the enthalpies and the reactivity of metal ions without any solvent effects.

2.2.2 Level of Calculations

In this study, all calculations were performed with Gaussian 03 program package. For DFT calculations, the three parameter functional developed by Becke, which combines the Becke's [35] gradient-corrected exchange functional and the Lee-Yang-Parr [36] with part of the exact Hartree-Fock exchange energy, has been employed (denoted as B3LYP). B3LYP has been found well suited both for description of ion-molecule [37-39] complexes and for the study of inter- and intra-molecular hydrogen bonds [39-42].

The DFT optimizations of molecular geometries were carried out using the standard split valence 6-31G basis set augmented by diffuse functions (d, p). The exponents of all diffuse and polarization functions were used as implemented in Gaussian 03 and the described basis sets have been specified via 6-31++G(d,p) keywords.

Vibration frequencies are also calculated at B3LYP level to confirm that all the stationary points correspond to true minima on the potential energy surface. All frequency calculations are performed using numerical second derivatives and verified that all structures are true minima by frequency analysis and obtained all positive Hessian eigenvalue. Zero-point corrections are included in energies. DFT methods are known to have smaller basis set superposition errors (BSSE) than other theoretical methods such as MP2 [43]. Thus, combinations of DFT with large polarized basis functions guarantee the BSSE to be negligible [44]. Basis set superposition errors (BSSE) were estimated for the most and second most stable Thymine–M complexes through the counterpoise method [45] implemented in the Gaussian 03 code.

2.2.3 Definition of Interaction Energy

The interaction energies IE were determined as the difference between the optimized energy of the metal cation-base systems $E(B+M^+)$ and the sum of the energies of the base $E(B)$ and the metal cation $E(M^+)$:

$$IE = E(B + M^+) - [E(B) + E(M^+)] \quad \textbf{(2.15)}$$

3. RESULTS AND DISCUSSION

In the text, naming is done according to the following procedure. The capital **T** stands for thymine molecule, the number that follows **T**, stands for the number of the tautomer. The next letter defines the conformational preference of the hydrogen atom in that conformer. O or N is present to indicate from which atom a metal atom is bound. The last letter is given according to the M-O-C angle.

The molecules with the similar geometries for mono and bivalent metal ions are shown on the same figure. The bond lengths for different metal ions are given in different brackets on the figure. Bond distances are reported in angstroms. The values without bracket represent bond length between Li^+ and N or O atom. The values in {-} parenthesis represents Be^{+2} and the values in (-), [-], ((-)) and [[-]] stands for Na^+, K^+, Mg^{+2} and Ca^{+2} respectively.

3.1 T1

Molecule **T1** is the most common form of thymine. When the metal interaction is taken into consideration, four conformers can be obtained for **T1** (**T1_O10a**, **T1_O10b**, **T1_O8**, **T1_0**). The M-O10-C4 angle is found to be ~172° for structure **T1_O10a** and ~110° for structure **T1_O10b**.

Structure **T1_O10a** is the lowest energy conformer both for 1A group alkali metal ions and Ca^{+2} ion (Table 3.1.1 and Figure 3.1.1). For Be^{+2} and Mg^{+2} ions, structure **T1_O10b** became the lowest energy conformer (Figure 3.1.2). The **T1_O10b** conformer cannot be obtained for Li^+, Na^+, K^+, and Ca^{+2} ions. Be^{+2} is the only metal that exists both in **T1_O10a** and **T1_O10b** conformers. The energy difference between two conformers is found to be 13 kcal/mol. Both the transferred charge and the distance between metal and thymine during formation of complex is an indicator of binding strength between the cations and thymine. When the charges of two structures are compared, in **T1_O10b**, the charge on beryllium and O10 is +1.276, and -0.944 respectively corresponding charges in **T1_O10a** is +1.556 and -1.082

Table 3.1.1: Energies including ZPE corrections (Hartree), relative energies (kcal/mol), interaction energies (kcal/mol), BSSE corrected energies (Hartree), BSSE corrected relative energies (kcal/mol) and distances (Å) of structure **T1** for metals Li^{+}, Na^{+}, K^{+}, Be^{+2}, Mg^{+2}, Ca^{+2}.

Thymine	*Distance (Å)*	*E (Hartree)*	*ΔE (kcal/mol)*	*IE(kcal/mol)*	E_{BSSE}	ΔE_{BSSE}
T1_O10a_Li	1.724	-461.4204	0.00	-50.25	-461.5369	0.00
T1_O8_Li	1.729	-461.4166	2.38	-47.88	-461.5328	2.56
T1_0_Li	-	-461.3647	34.95	-15.30		
T1_O10a_Na	2.098	-616.1947	0.00	-36.21	-616.3094	0.00
T1_O8_Na	2.104	-616.1917	1.88	-34.33	-616.3062	1.99
T1_O10a_K	2.495	-1053.8220	0.00	-25.84	-1053.9372	0.00
T1_O8_K	2.503	-1053.8194	1.58	-24.25	-1053.9344	1.70
T1_O10b_Be	1.454	-468.1155	0.00	-255.70	-468.2324	0.00
T1_O10a_Be	1.365	-468.0948	13.00	-242.70	-468.2122	12.70
T1_O8_Be	1.376	-468.0790	22.92	-232.78		
T1_0_Be	-	-468.0261	56.12	-199.58		
T1_O10b_Mg	1.864	-653.5094	0.00	-141.97	-653.6245	0.00
T1_O8_Mg	1.824	-653.4945	9.40	-132.57	-653.6089	9.81
T1_0_Mg	-	-653.4298	49.94	-92.02		
T1_O10a_Ca	2.140	-1131.0698	0.00	-92.31	-1131.1854	0.00
T1_O8_Ca	2.149	-1131.0615	5.24	-87.07	-1131.1767	5.46
T1_0_Ca	-	-1130.9928	48.29	-44.02		

respectively. When the distances are taken into consideration, Be-O10 distance is 1.4540 Å in **T1_O10b**, the corresponding distance in **T1_O10a** is 1.3651 Å. It is also noteworthy to mention that, the distance between beryllium ion and C11 is 1.8713 Å, which is an indicator of an interaction between those two atoms. **T1_O8** is always the second lowest energy conformer for all of the metals except Be^{+2}. Although the relative energy between **T1_O10** and **T1_O8** is 1.5-2.3 kcal/mol for group 1A metals, the value is increased up to 22.9 kcal/mol for Be^{+2}, 9.4 kcal/mol for Mg^{+2} and 5.2 kcal/mol for Ca^{+2}.

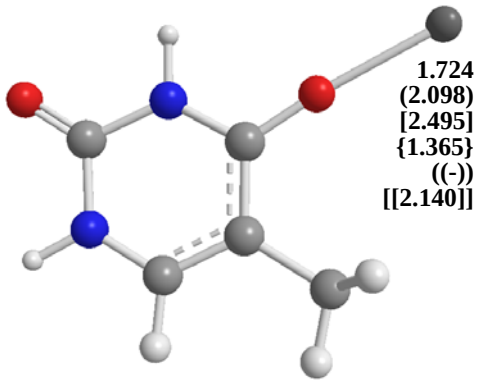

Figure 3.1.1: Structure **T1_O10a** with metals Li^{+}, Na^{+}, K^{+}, Be^{+2}, Ca^{+2}.

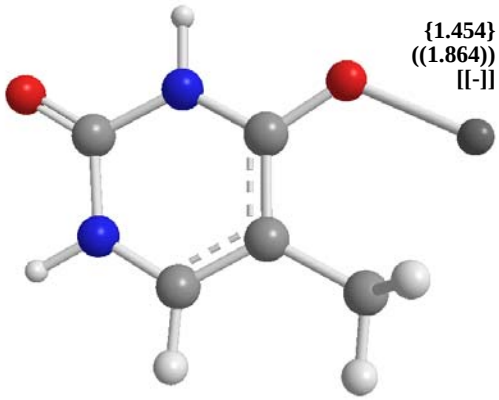

Figure 3.1.2: Structure **T1_O10b** with metals Be^{+2}, Mg^{+2}.

The canonical thymine **T1** has only monodentate binding sites for planar structures. The position of an ion in the global minimum of **T1** remains the same, i.e. the metal ions favor the same binding site independently the type of metal ion. For **T1**, it is found that monodentate binding from O10 is preferable to the same binding motif from O8 (Figure 3.1.1 and Figure 3.1.3). Our calculated atomic charges showed that both of the oxygen atoms in thymine are almost equally charged, while the three hydrogen atoms attached to C11 (methyl group hydrogens) are less positively charged than the hydrogen atom (H7 for **T1**) attached to N1. Thus, the repulsion between metal ion and the hydrogen atoms attached to the C11 will be weaker than that for the hydrogen atom attached to N1. This might be the reason for a stronger metal binding in **T1_O10a** than in **T1_O8.**

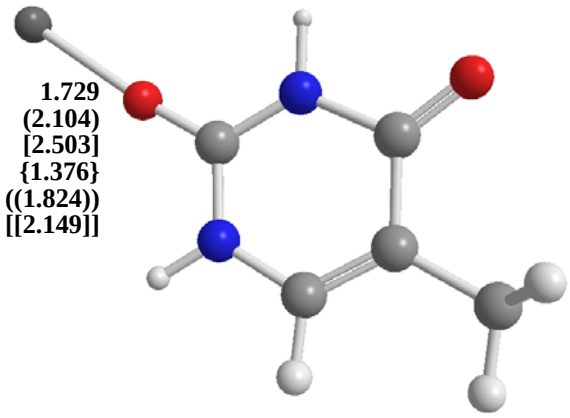

Figure 3.1.3: Structure **T1_O8** with metals Li^{+}, Na^{+}, K^{+}, Be^{+2}, Mg^{+2}, Ca^{+2}.

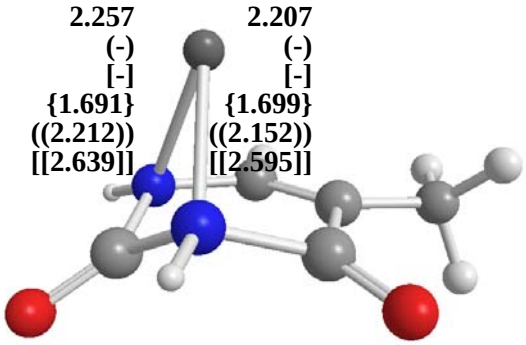

Figure 3.1.4: Structure **T1_0** with metals Li^{+}, Be^{+2}, Mg^{+2}, Ca^{+2}.

Although beryllium and lithium are the same row elements in the periodic table, interaction distances in the Be^{+2} complexes are shorter by ~0.4 Å than the corresponding Li^{+} complexes. This can be explained by the fact that Be-thymine interaction is stronger (-255.69 kcal/mol) than the one for Li-thymine (-50.0 kcal/mol) as shown in Table 3.1.1. This result is also true for Na^{+}-Mg^{+2}, K^{+}-Ca^{+2} comparatively. These results suggest that the size of a cation is vital for its binding with thymine.

Li^{+}, Be^{+2}, Mg^{+2} and Ca^{+2} are capable of forming cation-π complexes with the canonical form of the thymine **T1**. The **T1_0** structures are the least stable structures among **T1** conformers, in which, the planarity of ring structure is distorted from its original position and allowing cation-π complexes with nitrogens (N1 and N3) of the thymine base (Figure 3.1.4).

The binding energies are summarized in Table 3.1.1. The cation-π binding strengths are very strong in comparison with the common intermolecular interaction, e.g., hydrogen bonding that is normally no stronger than -20 kcal/mol. The IE values of Be^{+2}, Mg^{+2}, Ca^{+2} and Li^{+} with thymine are -255.69, -92.02, -44.01, -15.30 respectively, almost as strong as the binding between benzene and these cations. Among them, beryllium complexes have the strongest binding strength while lithium complexes have the weakest. Our results are in accordance with previous theoretical results [18].

3.2 T1_Me

The canonical thymine **T1** has been methylated from N1 site and the optimized **T1_Me** molecule is obtained. Although its electronic energy including ZPE is

decreased by 39 hartree, most of the structural and the electronic properties of **T1_Me** are in harmony with **T1**. There are five optimized structures for **T1_Me** (**T1_Me_O10a**, **T1_Me_O10b**, **T1_Me_O10c**, **T1_Me_ 2**, **T1_Me_ 3**). **T1_Me_O10a** is the lowest energy conformer for 1A group alkali metals and for calcium ion (Table 3.2.1 and Figure 3.2.1).

In case of Be^{+2} and Mg^{+2} ions, **T1_Me_O10b** became the lowest energy conformer (Figure 3.2.2). Different from the conformers in **T1**, a new conformer, in which, Mg^{+2} is nonlinearly bound to O10 is found. The planarity is distorted by 47° in M-O10-C4-C5 dihedral relative to O10a and O10b binding motifs. This structure is named as **T1_Me_O10c**, which is the second lowest energy conformer. Although the relative energy between **T1_Me_O10** and **T1_Me_O8** is 3-4 kcal/mol for group 1A metals, the value is increased up to 26.3 kcal/mol for Be^{+2}, 12.7 kcal/mol for Mg^{+2} and 8.9 kcal/mol for Ca^{+2}.

Table 3.2.1: Energies including ZPE corrections (Hartree), relative energies (kcal/mol), interaction energies (kcal/mol) and distances (Å) of methylated structure **T1_Me** for metals Li^{+}, Na^{+}, K^{+}, Be^{+2}, Mg^{+2}, Ca^{+2}.

Thymine	*Distance (Å)*	*E(Hartree)*	*ΔE(kcal/mol)*	*IE(kcal/mol)*
T1_Me_O10a_Li	1.718	-500.7080	0.00	-52.87
T1_Me_O8_Li	1.724	-500.7020	4.29	-48.58
T1_Me_0_Li	-	-500.6530	34.96	-17.91
T1_Me_O10a_Na	2.092	-655.4820	0.00	-38.41
T1_Me_O8_Na	2.101	-655.4760	3.70	-34.71
T1_Me_O10a_K	2.485	-1093.1100	0.00	-27.69
T1_Me_O8_K	2.499	-1093.1000	3.34	-24.35
T1_Me_O10b_Be	1.451	-507.4130	0.00	-264.51
T1_Me_O10a_Be	1.362	-507.3930	13.05	-251.46
T1_Me_O8_Be	1.377	-507.3710	26.37	-238.14
T1_Me_0_Be	-	-507.3280	53.59	-210.92
T1_Me_O10b_Mg	1.861	-692.8040	0.00	-148.89
T1_Me_O10c_Mg	1.813	-692.7990	3.09	-145.80
T1_Me_O8_Mg	1.833	-692.7840	12.72	-136.17
T1_Me_0_Mg	-	-692.7250	49.49	-99.40
T1_Me_O10a_Ca	2.133	-1170.3600	0.00	-97.62
T1_Me_O8_Ca	2.143	-1170.3500	8.92	-88.71
T1_Me_0_Ca	-	-1170.2800	48.71	-48.91

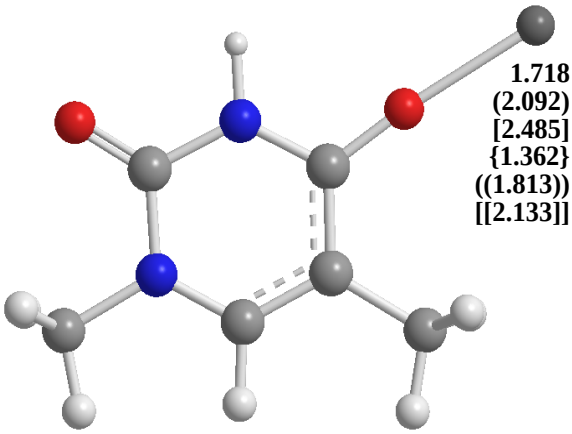

Figure 3.2.1: Structures **T1_Me_O10a** with metals Li^{+}, Na^{+}, K^{+}, Be^{+2}, Ca^{+2} and **T1_Me_O10c** with Mg^{+2}

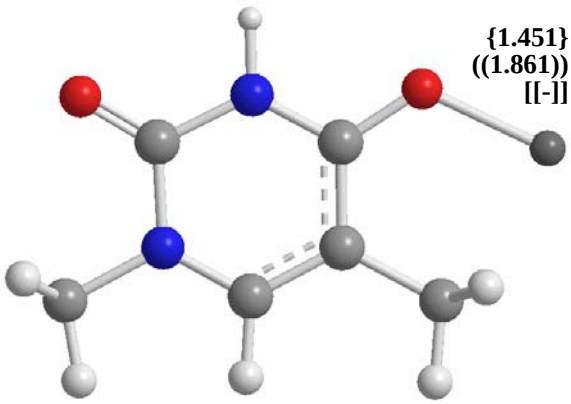

Figure 3.2.2: Structure **T1_Me_O10b** with metals Be^{+2}, Mg^{+2}.

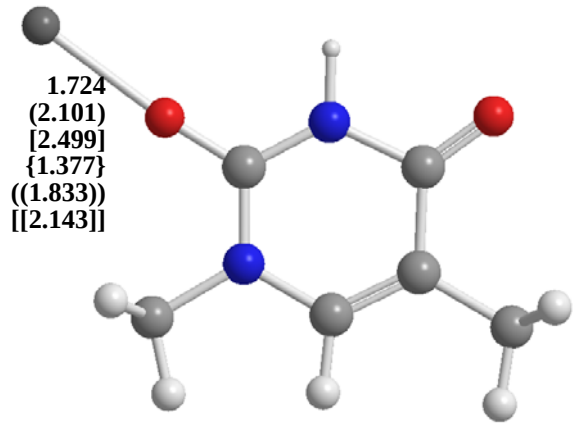

Figure 3.2.3: Structure **T1_Me_O8** with metals Li^{+}, Na^{+}, K^{+}, Be^{+2}, Mg^{+2}, Ca^{+2}.

Except cation-π complexes, only monodentate bindings can be modeled both for **T1** and **T1_Me**. It is found that similar charge distributions exist on both of the **T1** and methylated **T1**. Consequently, the global minimum is found when the ions favor M-O10 binding site rather than at M-O8, independent from the type of ions. Our calculated atomic charges showed that the two oxygen atoms in **T1_Me** thymine are almost equally charged as in **T1**. Although the hydrogen atoms on C7 and C11 have equal charges, the energy difference between **T1_Me_O10** and **T1_Me_O8** is increased due to steric hindrance created by the addition of methyl group on N1.

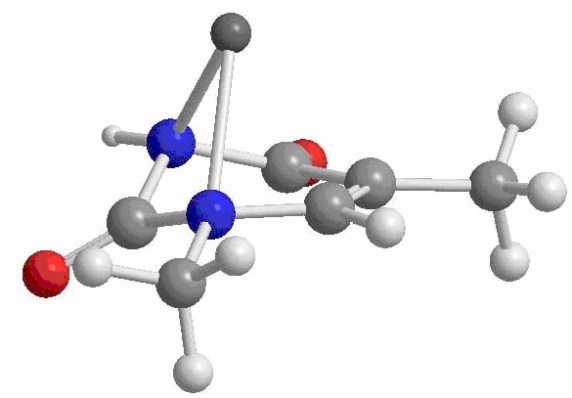

Figure 3.2.4: Structure **T1_Me_0** with metals Li^{+}, Be^{+2}, Mg^{+2}, Ca^{+2}.

Despite the fact that the shorter distances between metal ions and heteroatoms is an indicator of stronger interaction, the Be-O10 distance in the most stable conformer **T1_Me_O10b** (1.451 Å) is longer than the corresponding distance in **T1_Me_O10a** (1.361 Å) . This can be rationalized by the change in charge distributions. When the charges of two structures are compared, in **T1_Me_O10b**, the charge on beryllium and O10 is +0.762, and-0.176 respectively where in **T1_Me_O10a** charges are changed to +0.237 and +0.513 respectively.

Just like **T1**, the least stable conformer is **T1_Me_0** in which the planarity is distorted by the interaction of Li^{+}, Be^{+2}, Mg^{+2} and Ca^{+2}(Figure 3.2.4) The interaction energies of **T1_Me** with metals are changed by 2-10 kcal/mol with respect to **T1**.

3.3 T2

Molecule **T2** is one of the enol tautomers of **T1** (Figure 1.2). Two main conformers, **T2a** and **T2b** of molecule **T2**, are defined according to the position of the hydrogen atom on O10. Structure **T2a_O8** is the lowest energy conformer for all alkali metals

and Be^{+2} (Table 3.3.1 and Figure 3.3.1). For metal ions Ca^{+2} and Mg^{+2}, **T2b_O8** structures are the lowest energy conformers (Table 3.3.1 and Figure 3.3.2). This can be explained by the differences in charges and interactions between atoms. The relative energies between the lowest energy structure of the two main conformers, **T2a** and **T2b**, are usually within a range of ±0-6 kcal/mol except for Be^{+2}, in which two conformers differ by 22.3 kcal/mol.

Table 3.3.1: Energies including ZPE corrections (Hartree), relative energies (kcal/mol), interaction energies (kcal/mol) , BSSE corrected energies (Hartree), BSSE corrected relative energies (kcal/mol) and distances (Å) of structure **T2** for metals Li^+, Na^+, K^+, Be^{+2}, Mg^{+2}, Ca^{+2}.

Thymine	*Distance(Å)*	*E(Hartree)*	*ΔE(kcal/mol)*	*IE(kcal/mol)*	E_{BSSE}	ΔE_{BSSE}
T2a_O8a_Li	1.851	-461.4187	0.00	-61.73	-461.5350	0.00
T2a_O8b_Li	1.746	-461.4174	0.80	-60.92	-461.5338	0.76
T2b_O8a_Li	1.898	-461.4168	1.16	-67.92		
T2a_O10a_Li	1.848	-461.3664	32.80	-28.93		
T2a_O8a_Na	2.197	-616.1916	0.00	-46.83	-616.3062	0.00
T2b_O8a_Na	2.262	-616.1903	0.80	-53.39	-616.3046	1.01
T2a_O10a_Na	2.227	-616.1450	29.23	-17.61		
T2a_O8a_K	2.556	-1053.8153	0.00	-34.25	-1053.9303	0.00
T2a_O8b_K	2.499	-1053.8152	0.04	-34.20	-1053.9303	0.04
T2b_O8a_K	2.642	-1053.8134	1.22	-40.39		
T2a_O10a_K	2.685	-1053.7754	25.05	-9.19		
T2a_O8a_Be	1.518	-468.1397	0.00	-283.46	-468.2572	0.00
T2a_O8b_Be	1.370	-468.1080	19.91	-263.56	-468.2255	19.89
T2b_O8b_Be	1.378	-468.1042	22.31	-268.51		
T2b_O10a_Be	1.690	-468.0959	27.53	-263.29		
T2a_O10b_Be	1.582	-468.0352	65.57	-217.89		
T2a_O10a_Be	1.483	-468.0297	69.07	-214.40		
T2a_0_Be	-	-468.0160	77.65	-205.82		
T2b_0_Be	-	-468.0059	83.95	-206.87		
T2b_O8a_Mg	1.960	-653.5462	0.00	-184.97	-653.6619	0.00
T2a_O8a_Mg	1.929	-653.5375	5.43	-172.18	-653.6531	5.51
T2b_O10b_Mg	2.143	-653.5054	25.58	-159.40		
T2a_O10b_Mg	2.022	-653.4350	69.76	-107.86		
T2a_O10a_Mg	1.927	-653.4341	70.34	-107.28		
T2b_O8a_Ca	2.293	-1131.0942	0.00	-127.54	-1131.2097	0.00
T2a_O8a_Ca	2.247	-1131.0849	5.79	-114.39	-1131.2003	5.84
T2a_O8b_Ca	2.149	-1131.0778	10.28	-109.90		
T2a_O10a_Ca	2.302	-1130.9943	62.65	-57.53		
T2a_O10b_Ca	2.348	-1130.9912	64.65	-55.54		

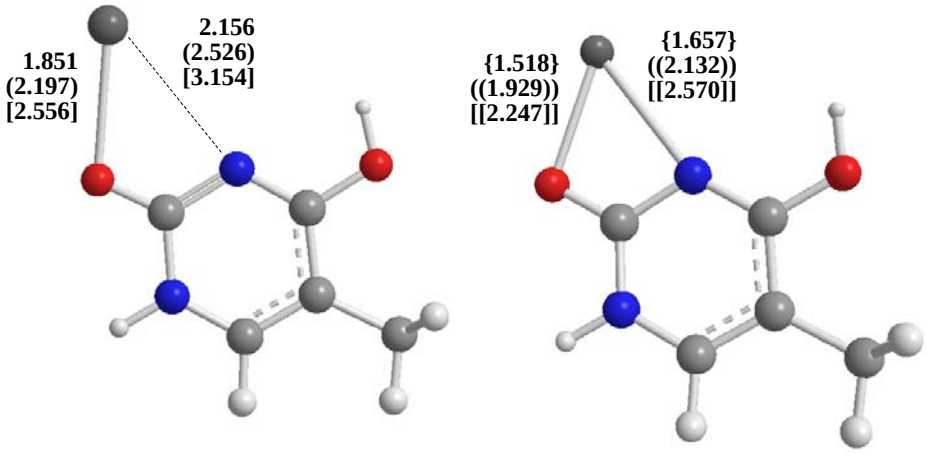

Figure 3.3.1 : Structure **T2a_O8a** with metals (a) Li^{+}, Na^{+}, K^{+} (b) Be^{+2}, Mg^{+2}, Ca^{+2}.

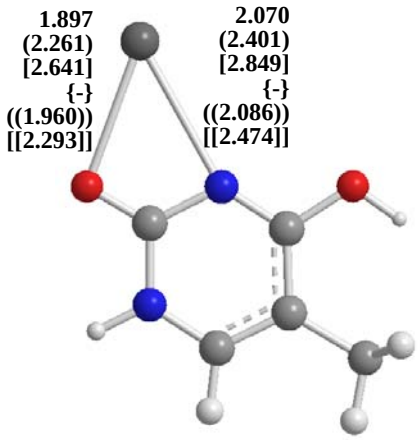

Figure 3.3.2 : Structure **T2b_O8a** with metals Li^{+}, Na^{+}, K^{+}**,** Mg^{+2}, Ca^{+2}.

For all cases, the bidentate binding motif O8-M-N3 is preferable to the monodentate one due to the stability of the structures. Both for the alkali and alkaline earth metals binding tendencies are the same. Despite the fact that beryllium is a divalent metal, charge on beryllium in **T2a_O8,** is +1.343. But for magnesium and calcium, the APT charges are +1.557 and +1.792 respectively. For **T2a_O8**, those much positive charges on metal atoms may cause a destabilizing interaction with a hydrogen atom which has a charge around +0.450. Thus Mg^{+2} and Ca^{+2} ions prefer the **T2b_O8** conformer.

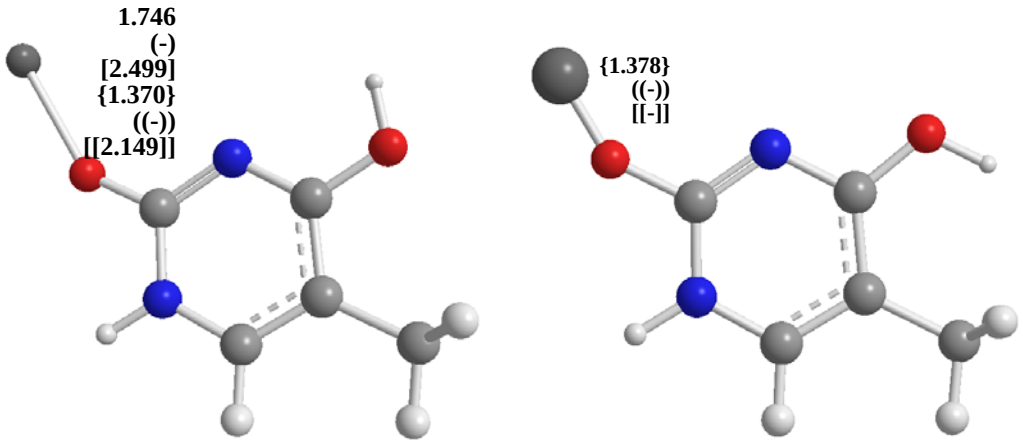

Figure 3.3.3: Structures **T2a_O8b** and **T2b_O8b** with metals Li^{+}, K^{+}, Be^{+2}, Ca^{+2} and with metal Be^{+2} respectively.

The second most stable structure for Li^{+}, K^{+}, Be^{+2} is **T2a_O8b**. The relative energies between **T2a_O8a** and **T2a_O8b** are found to be 0.80 kcal/mol and 0.04 kcal/mol for Li^{+} and K^{+} respectively which are negligibly small. The energy difference between monodentate and bidentate motifs of Be^{+2} and Ca^{+2} cations are 19 kcal/mol and 5 kcal/mol respectively. The difference can be explained by the bidentate binding preference of divalent metals.

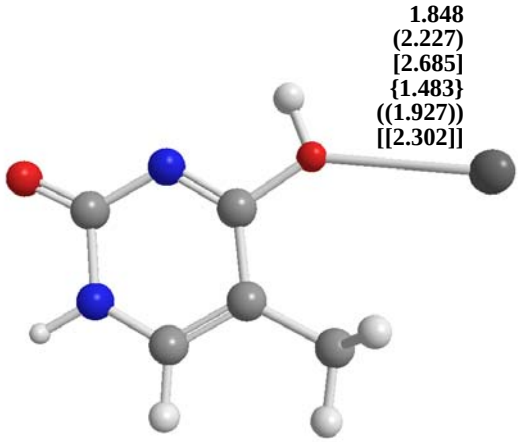

Figure 3.3.4: Structure **T2a_O10a** with metals Li^{+}, Na^{+}, K^{+}**,** Be^{+2}, Mg^{+2}, Ca^{+2}.

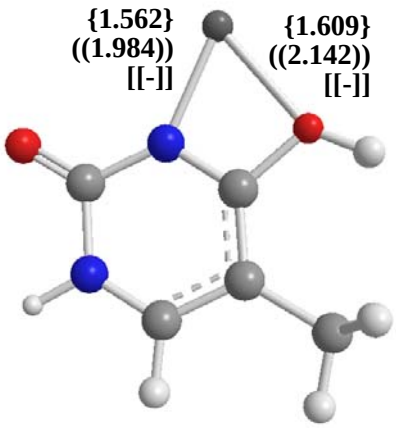

Figure 3.3.5: Structure **T2b_O10a** with Be^{+2} and **T2b_O10b** with Mg^{+2}.

For the interaction of metal atoms with oxygen atom, monovalent metal ions (Li^{+}, Na^{+}, K^{+}) bind directly and linearly to O10. For the divalent atoms there are two conformers that have to be taken into consideration. Those are named as **T2a_O10a** and **T2a_O10b**. The latter one is more stable than the former one, which can be explained by the preference of bidentate binding to monodentate binding. In **T2a_O10b**, the ring planarity negligibly distorted. It is noteworthy to state that methyl group on C5 is enormously distorted for Ca^{+2}, Mg^{+2}, Be^{+2} by 155.12°, -143°, -148° respectively (Figure 3.3.6).

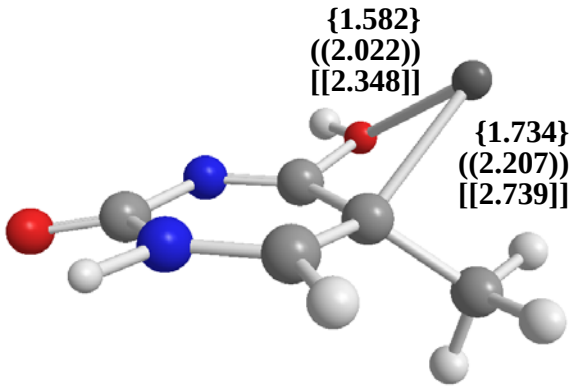

Figure 3.3.6: Structure **T2a_O10b** with metals Be^{+2}, Mg^{+2}, Ca^{+2}.

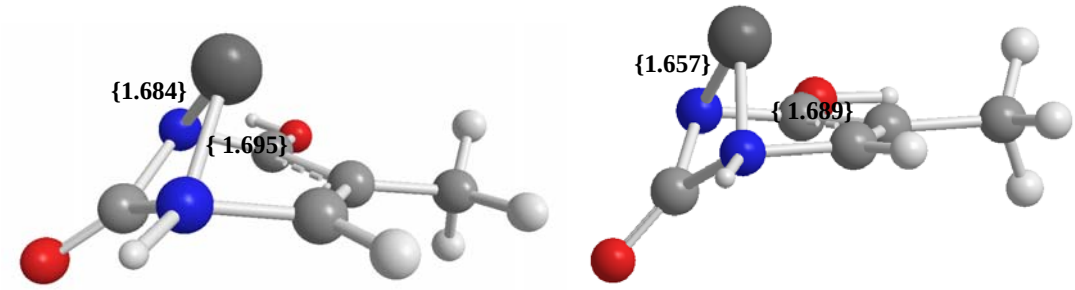

Figure 3.3.7: Structures **T2a_0** and **T2b_0** with metal Be^{+2}.

Only Be^{+2} is capable of forming cation-π complexes with the **T2** conformers, in which, the structure is distorted from its original position and allowing cation-π complexes with nitrogens (N1 and N3) of the base (Figure 3.3.7).

3.4 T2_Me

The enol tautomer **T2** has been methylated from N1 site and two main conformers, **T2a_Me** and **T2b_Me** are optimized. Although their electronic energies including ZPE are decreased by 39 hartree, most of the structural and the electronic properties of **T2a_Me** and **T2b_Me** are in accordance with **T2a** and **T2b** respectively. Conformer **T2a_Me_O8a** is the lowest energy conformer for all alkali metals (Table 3.4.1 and Figure 3.4.1). For alkali earth metals, **T2b_Me_O8** conformers are lowest energy structures (Table 3.4.1 and Figure 3.4.2).

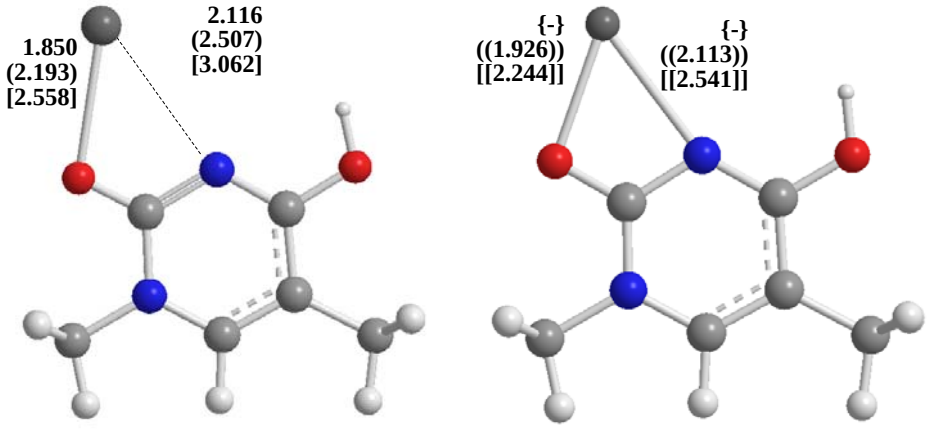

Figure 3.4.1 : Structure **T2a_Me_O8a** with metals (a) Li^{+}, Na^{+}, K^{+} (b) Mg^{+2}, Ca^{+2}.

Table 3.4.1: Energies including ZPE corrections (Hartree), relative energies (kcal/mol), interaction energies (kcal/mol) and distances (Å) of methylated structure **T2_Me** for metals Li^{+}, Na^{+}, K^{+}, Be^{+2}, Mg^{+2}, Ca^{+2}.

Thymine	*Distance(Å)*	*E(Hartree)*	*ΔE(kcal/mol)*	*IE(kcal/mol)*
T2a_Me_O8a_Li	1.850	-500.7073	0.00	-64.23
T2b_Me_O8a_Li	1.894	-500.7059	0.89	-70.56
T2a_Me_O10a_Li	1.844	-500.6549	32.91	-31.32
T2a_Me_O8a_Na	2.193	-655.4792	0.00	-48.69
T2b_Me_O8a_Na	2.259	-655.4784	0.52	-55.38
T2a_Me_O10a_Na	2.222	-655.4330	29.02	-19.67
T2a_Me_O8a_K	2.558	-1093.1019	0.00	-35.48
T2b_Me_O8a_K	2.641	-1093.1006	0.85	-41.84
T2a_Me_O10a_K	2.672	-1093.0628	24.56	-10.92
T2b_Me_O8b_Be	1.526	-507.4464	0.00	-304.46
T2a_Me_O8b_Be	1.371	-507.4011	28.42	-268.82
T2b_Me_O10_Be	1.603	-507.3955	31.89	-272.56
T2a_Me_O10b_Be	-	-507.3359	69.31	-227.93
T2a_Me_O10a_Be	1.483	-507.3262	75.42	-221.83
T2a_Me_0_Be	-	-507.3182	80.42	-216.83
T2b_Me_0_Be	-	-507.3080	86.84	-217.62
T2b_Me_O8a_Mg	1.956	-692.8418	0.00	-191.70
T2a_Me_O8a_Mg	1.926	-692.8329	5.58	-178.91
T2b_Me_O10_Mg	2.123	-692.8012	25.51	-166.19
T2a_Me_O10b_Mg	-	-692.7334	68.05	-116.44
T2a_Me_O10a_Mg	1.941	-692.7287	70.96	-113.54
T2b_Me_O8a_Ca	2.290	-1170.3869	0.00	-132.42
T2a_Me_O8a_Ca	2.244	-1170.3771	6.09	-119.12
T2a_Me_O10a_Ca	2.293	-1170.2869	62.75	-62.47

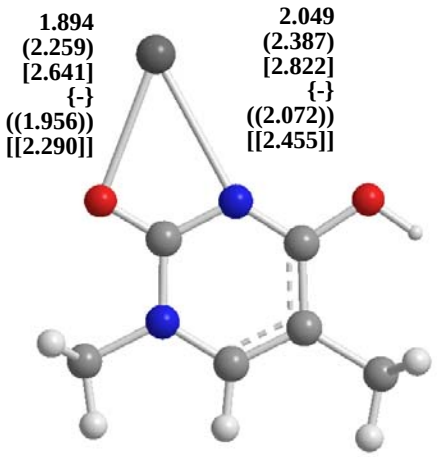

Figure 3.4.2: Structure **T2b_Me_O8a** with metals Li^{+}, Na^{+}, K^{+}, Mg^{+2}, Ca^{+2}.

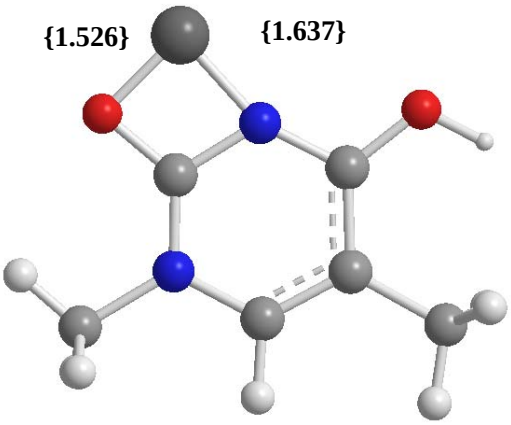

Figure 3.4.3: Structure **T2b_Me_O8b** with metal Be^{+2}.

Five metalated molecules can be modeled for **T2a_Me** (**T2a_Me_O8a**, **T2a_Me_O8b**, **T2a_Me_O10a, T2a_Me_O10b**, **T2a_Me_0**). For **T2a_Me**, both monodentate and bidentate binding motifs are found. The position of an ion in the global minimum of **T2a_Me** remains the same, i.e., the ions favor the same binding site independently the type of ion. In the case of **T2a_Me_O8a**, alkali metals and alkali earth metals (Mg^{+2} and Ca^{+2}) prefer bidentate like binding motif at O8-M-N3 which is more favorable than monodentate binding due to the stability of the structure (Figure 3.4.1). The conformer **T2a_Me_O8b** is obtained for only Be^{+2} (Figure 3.4.4).

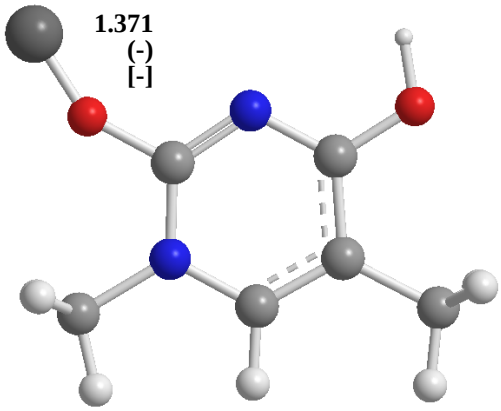

Figure 3.4.4: Structure **T2a_Me_O8b** with metal Be^{+2}.

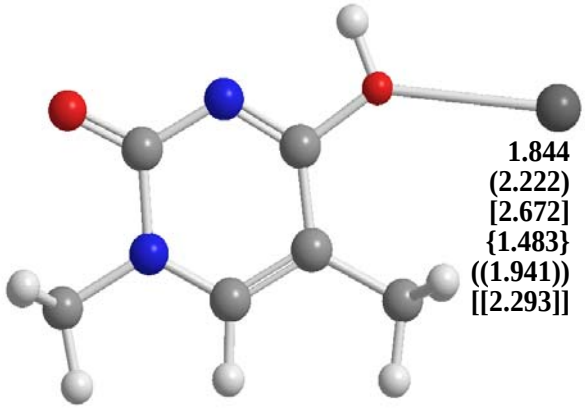

Figure 3.4.5: Structure **T2a_Me_O10a** with metals Li^{+}, Na^{+}, K^{+}, Be^{+2}, Mg^{+2}, Ca^{+2}.

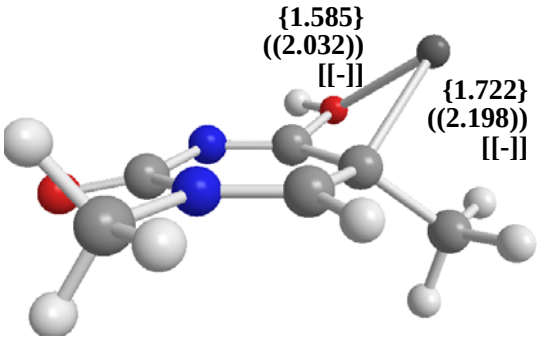

Figure 3.4.6: Structure **T2a_Me_O10b** with metals Be^{+2}, Mg^{+2}.

In case of **T2_Me**, the same binding tendency is observed for O10-metal interaction just as **T2.** For Mg^{+}, metal binds nonlinearly to **T2a_Me_O10a**, where M-O10-C4-C5 dihedral is changed about 11° from its planar position. And there is one more structure that can be modeled for the M-O10 interaction is **T2a_Me_O10b,** where Be^{+2} and Mg^{+2} ions prefer to form a bidentate binding rather than monodentate. The M-O10-C4-C5 dihedral changed to 15.7° and 29° for Be^{+2} and Mg^{+2} respectively, where the planarity is distorted (Figure 3.4.5 and Figure 3.4.6).

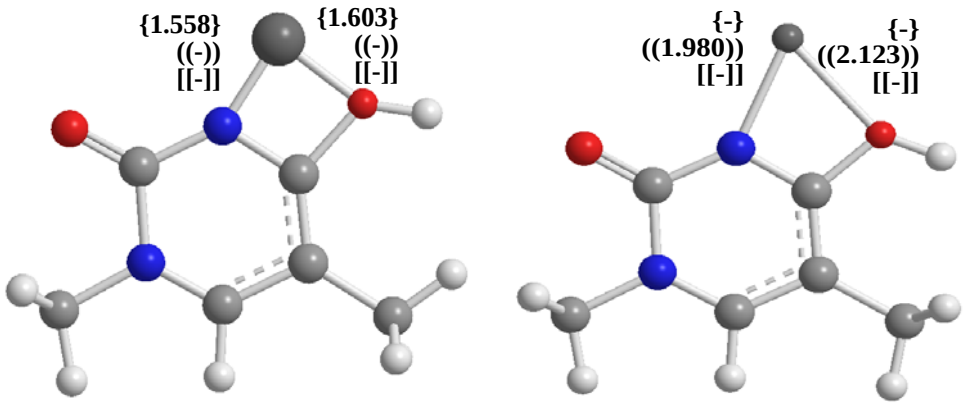

Figure 3.4.7: Structure **T2b_Me_O10** with Be^{+2} and Mg^{+2}.

Four metalated molecules are modeled for **T2b_Me** (**T2b_Me_O8a**, **T2b_Me_O8b**, **T2b_Me_O10, T2b_Me_0**). Just like **T2b**, in **T2b_Me** structure, all metals prefer bidentate position at M-O8 rather than at M-O10. The lowest energy conformer is **T2b_Me_O8a** for all **T2b**-M structures except Be^{+2} ion. The beryllium ion prefers **T2b_Me_O8b** conformer that can be obtained by the rotation of methyl group on N1. (Figure 3.4.2 and Figure 3.4.3)

The **T2b_Me_O10** cannot be obtained for monovalent atoms and Ca^{+2}. In **T2b_Me_O10_Mg**, the methyl group attached to C5 is rotated by 51° with respect to beryllium complex of the same structure (Figure 3.4.7).

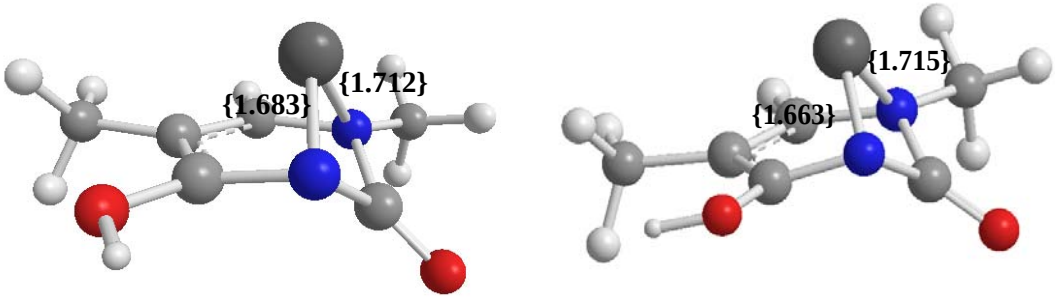

Figure 3.4.8: Structures **T2a_Me_0** and **T2b_Me_0** with metal Be^{+2}.

Likewise **T2a** and **T2b**, only Be^{+2} is capable of forming cation-π complexes with the **T2a_Me** and **T2b_Me**, in which, the structure is distorted from its original position and allowing a cation-π complex with nitrogens (N1 and N3) of the base as usual (Figure 3.4.8).

3.5 T3

Molecule **T3** is the highest energy enol tautomer of canonical structure **T1**. In **T3a**, N3-C2-O8-H dihedral angle is -0.010˚ where the value is an indication of planarity. In **T3b**, the N3-C2-O8-H dihedral angle is no longer planar (-166.45°) when no metal-thymine interaction is present. In **T3**, metals preferred bidentate position at M-O10 rather than at M-O8 as expected. Structure **T3a_M** is the lowest energy conformer for all alkali metals and beryllium. (Table 3.5.1 and Figure 3.5.1). The overall energy of **T3b_O10a_Mg** is lower **T3a_O10a_Mg** by 1.82 kcal/mol (Table 3.5.1 and Figure 3.5.1-3.5.2). In case of Ca^{+2}, the overall energy of **T3b_O10a** is lower **T3a_O10a** by 2.15 kcal/mol. The relative energies between the lowest energy structure of the two main conformers, **T3a** and **T3b**, are usually within a range of

1.8-4.4 kcal/mol for both alkali and alkaline earth metals except for Be^{+2} where the difference is 22.5 kcal/mol.

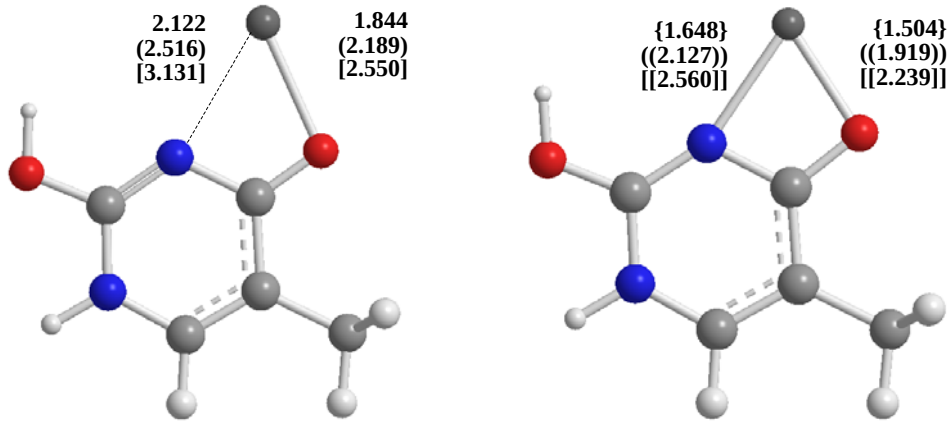

Figure 3.5.1: Structure **T3a_O10a** with metals (a) Li^{+}, Na^{+}, K^{+} (b) Be^{+2}, Mg^{+2}, Ca^{+2}

Table 3.5.1: Energies including ZPE corrections (Hartree), relative energies (kcal/mol), interaction energies (kcal/mol), BSSE corrected energies (Hartree), BSSE corrected relative energies (kcal/mol) and distances (Å) of structure **T3** for metals Li^{+}, Na^{+}, K^{+}, Be^{+2}, Mg^{+2}, Ca^{+2}.

Thymine	*Distance(Å)*	*E(Hartree)*	*ΔE(kcal/mol)*	*IE(kcal/mol)*	E_{BSSE}	ΔE_{BSSE}
T3a_O10a_Li	1.844	-461.4136	0.00	-64.42	-461.5296	0.00
T3a_O10b_Li	1.736	-461.4116	1.23	-63.18	-461.5278	1.16
T3b_O10a_Li	1.885	-461.4069	4.22	-70.12		
T3a_O10a_Na	2.189	-616.1856	0.00	-48.95	-616.2998	0.00
T3b_O10a_Na	2.240	-616.1794	3.93	-54.95	-616.2928	4.42
T3a_O10b_K	2.486	-1053.8084	0.00	-35.77	-1053.9229	0.00
T3a_O10a_K	2.550	-1053.8083	0.05	-35.72	-1053.9232	-0.14
T3b_O10a_K	2.619	-1053.8014	4.40	-41.29		
T3a_O10a_Be	1.504	-468.1438	0.00	-291.86	-468.2608	0.00
T3a_O10c_Be	1.436	-468.1215	13.96	-277.90	-468.2385	13.99
T3a_O10b_Be	1.361	-468.1141	18.61	-273.25		
T3b_O10c_Be	1.433	-468.1078	22.54	-279.24		
T3b_O10b_Be	1.368	-468.1049	24.37	-277.41		
T3b_O8_Be	1.670	-468.0664	48.52	-253.26		
T3a_0_Be	-	-468.0148	80.90	-210.96		
T3b_O10a_Mg	1.947	-653.5403	0.00	-189.70	-653.6555	0.00
T3a_O10a_Mg	1.919	-653.5374	1.82	-177.96	-653.6527	1.76
T3a_O10c_Mg	1.838	-653.5102	18.88	-160.90		
T3b_O10c_Mg	1.832	-653.4969	27.21			
T3a_O8_Mg	2.043	-653.3956	90.78	-89.00		
T3b_O10a_Ca	2.278	-1131.0853	0.00	-130.40	-1131.2001	0.00
T3a_O10a_Ca	2.239	-1131.0819	2.15	-118.32	-1131.1969	2.06
T3a_O10b_Ca	2.133	-1131.0759	5.91	-114.56		

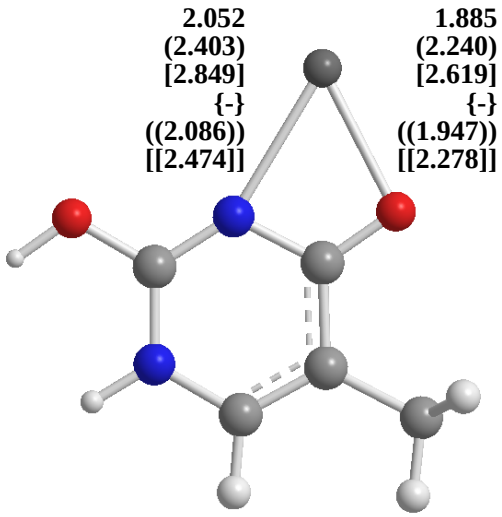

Figure 3.5.2 : Structure **T3b_O10a** with metals Li^{+}, Na^{+}, K^{+}, Mg^{+2}, Ca^{+2}

For **T3a**, both monodentate and bidentate binding motifs are modeled (Figure 3.5.1-Figure 3.5.3 and Figure 3.5.4). Three different conformers are found for the interactions of metals with O10. **T3a_O10a** is the lowest energy conformer for all metals except K^{+}. The **T3a_O10b** is modeled for Li^{+}, K^{+}, Be^{+2}, Ca^{+2} and the **T3a_O10c** can be optimized only for Be^{+2} and Mg^{+2}. In case of K^{+}, **T3a_O10b** is the most stable conformer.

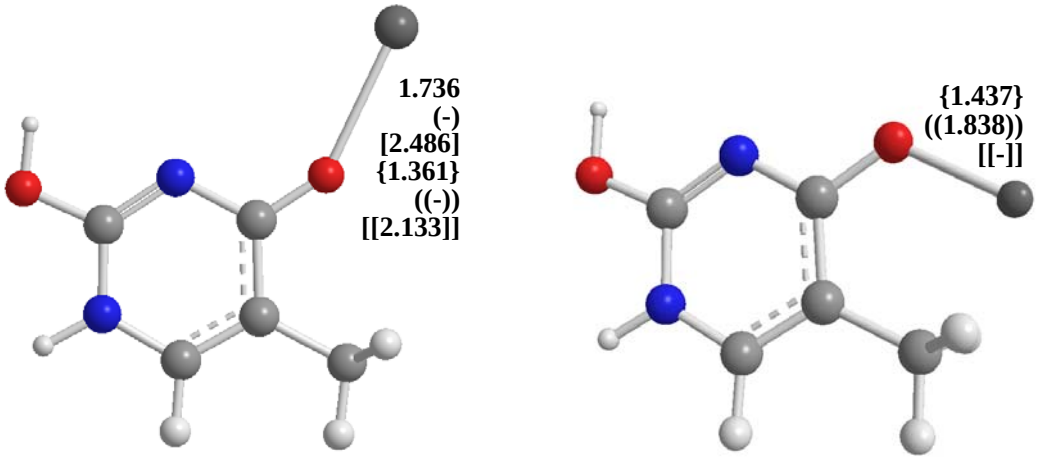

Figure 3.5.3: Structures (a) **T3a_O10b** with metals Li^{+}, K^{+}, Be^{+2}, Ca^{+2} (b) **T3a_O10c** with metals Be^{+2}, Mg^{+2}.

For the ions Li^{+} and K^{+}, the relative energy between **T3a_O10a** and **T3a_O10b** complexes is small. For the case of divalent atoms, Be^{+2}, Mg^{+2} and Ca^{+2}, bidentate binding motif O10-M-N3 is observed in **T3a_O10a** which is more favorable than monodentate binding (**T3a_O10b** and **T3a_O10c**) due to stability of the structure.

An increase in relative energy between **T3a_O10a** and **T3a_O10b-c** for divalent atoms can be attributed to this fact. Although both **T3a_O10c** and **T3a_O10b** have monodentate binding motif for beryllium, the distance between metal and O10 atom differ by 0.076 Å. For Be^{+2}, the **T3a_O10c** is more stable than **T3a_O10b** by 5 kcal/mol. This fact can be rationalized by the ability of **T3a_O10c** forming a six-membered ring like structure. From NBO calculations, it is found that there exists a donation from C11-H_a (12,68) and C11-H_b (12,59) bonds to beryllium which brings an extra stability to the structure. In **T3a_O8**, metal-O8 interaction is not favorable for Mg^{+2}. The energy difference between this conformer and the lowest energy one is 90.7 kcal/mol (Figure 3.5.4).

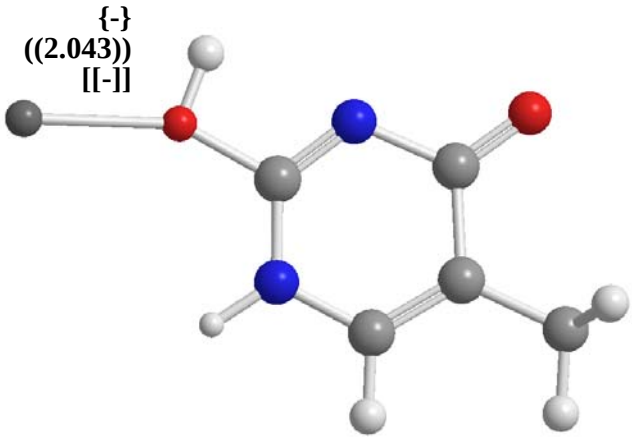

Figure 3.5.4: Structure **T3a_O8** with metal Mg^{+2}.

It is found that, alkali and alkaline earth metals can interact with conformer **T3b** in form of bidentate binding motif O8-M-N3 in **T3b_O10a** which is more favorable than monodentate binding due to the stability of the structure. (Figure 3.5.2). This is not true for the case of Be^{+2} in which monodentate binding motifs **T3b_O10c** and **T3b_O10b** can be obtained (Figure 3.5.5). The **T3b_O10a** complex with Mg^{+2} ion is more stable than the bidentate binding motif O10-M-N3 of **T3a** by 1.8 kcal/mol.

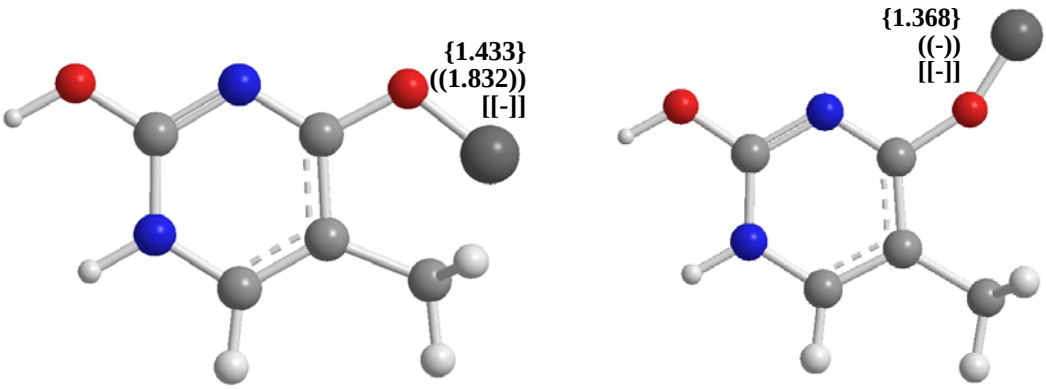

Figure 3.5.5: Structures (a) **T3b_O10c** with metals Be^{+2} and Mg^{+2} (b) **T3b_O10b** with metal Be^{+2}.

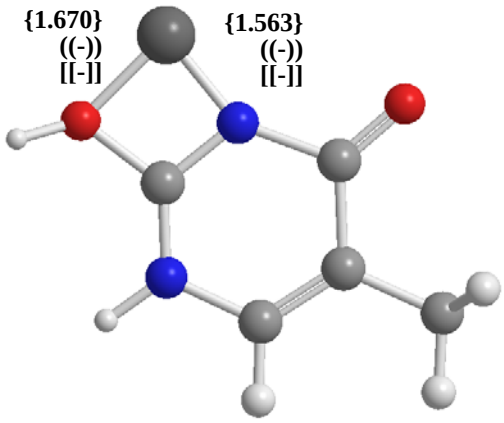

Figure 3.5.6: Structure **T3b_O8** with metal Be^{+2}.

The **T3b_O8** structure can be optimized with only Be^{+2} metal which is higher in energy than the other **T3**-Be structures. The relative energy between the most stable structure **T3a_O10a_Be** and **T3b_O8_Be** is 81kcal/mol. In this structure, the H11-O8-C2-N1 dihedral angle is changed from planarity to 30˚ and a bidentate binding O8-M-N3 motif is seen for Be^{+2}. (Figure 3.5.6).

Only Be^{+2} is capable of forming cation-π complexes with the **T3a**, in which, the structure is distorted from its original position with 36.7° and allowing a binding with only nitrogen (N3) of the base (Figure 3.5.7).

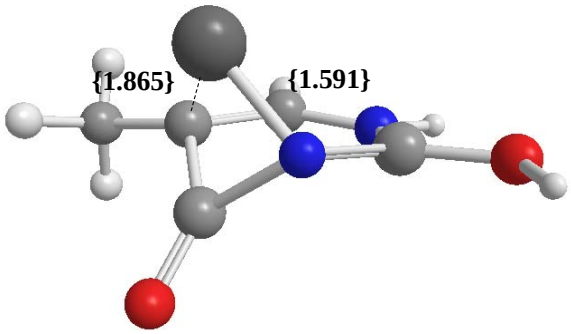

Figure 3.5.7: Structure **T3a_0** with metal Be^{+2}.

3.6 T3_Me

The enol tautomer **T3** has been methylated from N1 site and two main conformers, **T3a_Me** and **T3b_Me** are obtained just as **T3a** and **T3b**. Although their electronic energies including ZPE are decreased by 39 hartree, most of the structural and the electronic properties of **T3a_Me** and **T3b_Me** are in accordance with **T3a** and **T3b** respectively. Structure **T3a_Me** is the lowest energy conformer for all alkali metals and Be^{+2} (Table 3.6.1 and Figure 3.6.1). For Mg^{+2} and Ca^{+2}, **T3b_Me_O10a** structure is the lowest energy conformers (Table 3.6.1 and Figure 3.6.2).

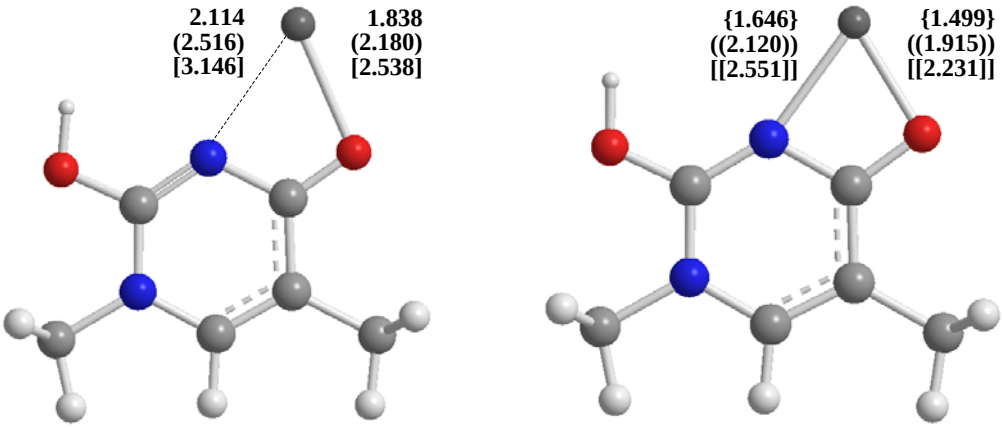

Figure 3.6.1: Structure **T3a_Me_O10a** with metals (a) Li^{+}, Na^{+}, K^{+} (b) Be^{+2}, Mg^{+2}, Ca^{+2}.

Table 3.6.1: Energies including ZPE corrections (Hartree), relative energies (kcal/mol), interaction energies (kcal/mol) and distances (Å) of methylated structure **T3_Me** for metals Li^{+}, Na^{+}, K^{+}, Be^{+2}, Mg^{+2}, Ca^{+2}.

Thymine	*Distance (Å)*	*E(Hartree)*	*ΔE(kcal/mol)*	*IE(kcal/mol)*
T3a_Me_O10a_Li	1.838	-500.7008	0.00	-67.11
T3a_Me_O10b_Li	1.729	-500.6988	1.23	-65.88
T3b_Me_O10a_Li	1.877	-500.6939	4.30	-73.09
T3b_Me_O10b_Li	1.725	-500.6862	9.16	-68.24
T3a_Me_O8a_Li	1.842	-500.6276	45.92	-21.18
T3a_Me_O10a_Na	2.180	-655.4721	0.00	-51.22
T3b_Me_O10a_Na	2.238	-655.4657	4.00	-57.52
T3a_Me_O8a_Na	2.231	-655.4083	40.02	-11.20
T3a_Me_O10b_K	2.473	-1093.0943	0.00	-37.66
T3a_Me_O10a_K	2.538	-1093.0941	0.07	-37.59
T3b_Me_O10a_K	2.611	-1093.0871	4.49	-43.46
T3a_Me_O10a_Be	1.499	-507.4413	0.00	-301.06
T3a_Me_O10c_Be	1.434	-507.4183	14.42	-286.65
T3a_Me_O10b_Be	1.358	-507.4105	19.31	-281.75
T3b_Me_C2C4_Be	1.431	-507.4036	23.67	-287.68
T3b_Me_O10b_Be	1.365	-507.4004	25.68	-285.68
T3b_Me_O8_Be	1.555	-507.3658	47.39	-263.97
T3b_Me_O10a_Mg	1.942	-692.8345	0.00	-197.19
T3a_Me_O10a_Mg	1.915	-692.8315	1.87	-185.04
T3a_Me_O10c_Mg	1.836	-692.8040	19.11	-167.79
T3a_Me_O8b_Mg	2.029	-692.6911	90.01	-96.89
T3b_Me_O10a_Ca	2.272	-1170.3772	0.00	-136.47
T3a_Me_O10a_Ca	2.231	-1170.3736	2.31	-123.87
T3a_Me_O10b_Ca	2.125	-1170.3672	6.28	-119.90

In the case of **T3_Me**, metals prefer bidentate position at M-O10 rather than at M-O8 as expected. The relative energies between the lowest energy structure of the two main conformers, **T3a_Me** and **T3b_Me,** are usually within a range of 1-4 kcal/mol for alkali metals, Mg^{+2} and Ca^{+2}.

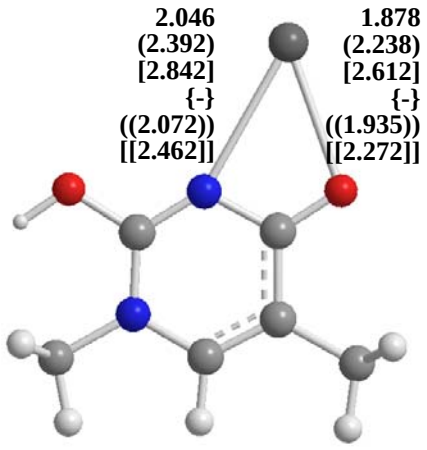

Figure 3.6.2: Structure **T3b_Me_O10a** with metals Li^{+}, Na^{+}, K^{+},Mg^{+2}, Ca^{+2}.

For **T3a_Me**, both monodentate and bidentate binding motifs can be obtained (Figure 3.6.1-3.6.3-3.6.4). The position of an ion in the global minimum of **T3a_Me** remains the same, i.e., the ions favor the same binding site independently the type of ion. Three different conformers can be modeled when ions interact with O10. **T3a_Me_O10a** is the lowest energy conformer for all metals except K^+.

In the case of **T3a_Me_O10a**, alkaline earth metals have bidentate binding with N3 and O10 but for alkali metals, there is an interaction with N3 (Figure 3.6.1). For the case of K^+, **T3a_Me_O10b** is the most stable conformer.

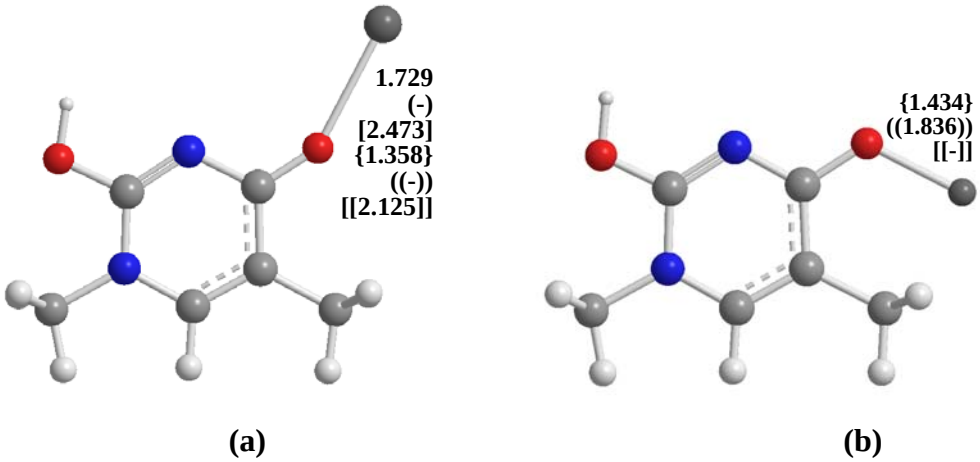

Figure 3.6.3: Structure (a) **T3a_Me_O10b** with metals Li^+, K^+, Be^{+2}, Ca^{+2} (b) **T3a_Me_O10c** with metals Be^{+2}, Mg^{+2}.

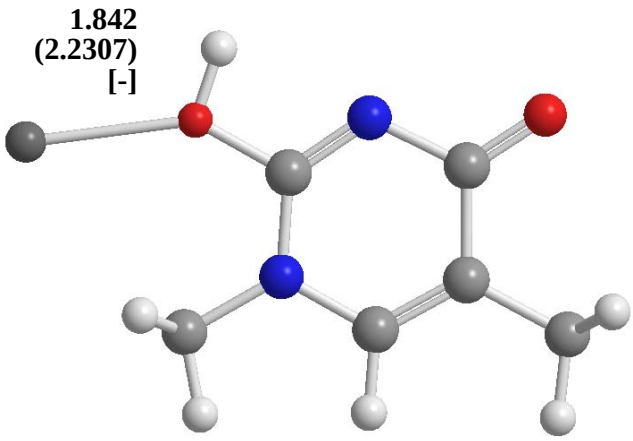

Figure 3.6.4: Structure **T3a_Me_O8a** with metals Li^+, Na^+.

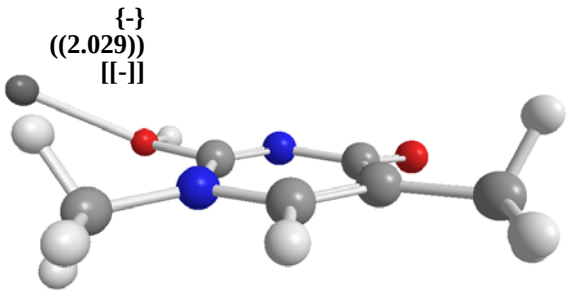

Figure 3.6.5: Structure **T3a_Me_O8b** with metal Mg^{+2}

In the case of Na^{+} and Mg^{+2}, the conformer **T3a_Me_O10b** can not be obtained. The **T3a_Me_O10c** is modeled for only Be^{+2} and Mg^{+2}. For the atoms on O8 two conformers are taken into account. **T3a_Me_O8a** is modeled for Li^{+} and Na^{+} in which the cations is located in the same plane of ring atoms. (Figure 3.6.4) **T3a_Me_O8b** is modeled for Mg^{+2} where metal binds with 33° difference in M16-O8-C4-C5 dihedral in which a distortion from the ring plane is observed (Figure 3.6.5).

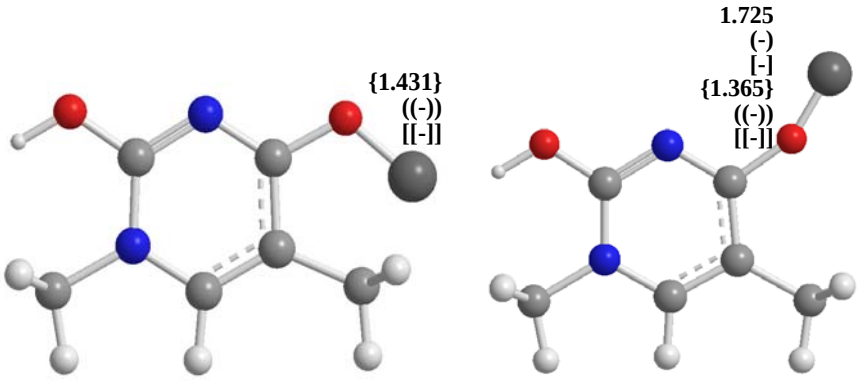

(a) **(b)**

Figure 3.6.6: Structures (a) **T3b_Me_O10c** with metal Be^{+2} and (b) **T3b_Me_O10b** with metals Li^{+}, Be^{2+}.

For **T3b_Me**, both monodentate and bidentate binding motifs can be modeled (Figure 3.6.2, Figure 3.6.6-3.6.7). In **T3b_Me**, bidentate position at M-O10 is preferable for metals. Both the monovalent and divalent atoms except Be^{+2} bidentate binding motif O10-M-N3 in **T3b_Me_O10a** is observed, which is more favorable than monodentate binding. The **T3b_Me_O10**a complexes formed with Mg^{+2} and Ca^{+2} are more stable than the bidentate binding motif O10-M-N3 of **T3a_Me**. Unlike **T3a_Me**, only for Li^{+} and Be^{+2} monodentate binding at M-O10 can be modeled (Figure 3.6.6). The conformer **T3b_Me_O10c** can only be modeled for Be^{+2} which is the lowest energy conformer for Be^{+2} (Figure 3.6.6).

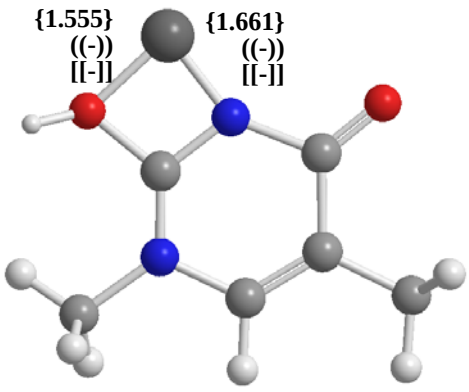

Figure 3.6.7: Structure **T3b_Me_O8** with metal Be^{+2}.

For **T3_Me-Be** complexes, **T3b_Me_O8** can be optimized with the lowest stability compared to the other **T3b_Me-Be** structures. The relative energy is 47 kcal/mol (Figure 3.6.7). It is only the case, in which, the cation-π complexes could not be found.

3.7 T4

Molecule **T4** is another enol tautomer of **T1**. There are two conformers **T4a** and **T4b** exist according to the position of the hydrogen atom on O8. Structure **T4a_O10** is the lowest energy conformer for all alkali and alkaline earth metals. (Table 3.7.1 and Figure 3.7.1-3.7.2). The relative energies between the lowest energy structure of the two main conformers, **T4a** and **T4b,** are usually within a range of 9-11 kcal/mol (Table 3.7.1).

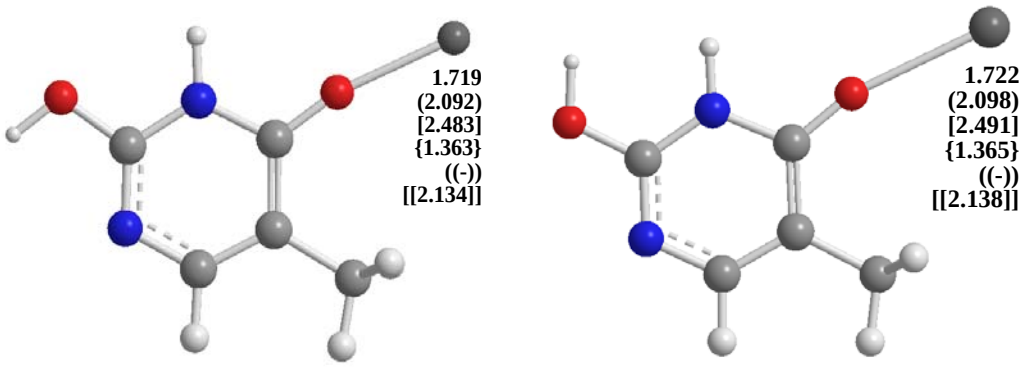

(a) **(b)**

Figure 3.7.1: Structures (a) **T4a_O10a** and (b) **T4b_O10a** with metals Li^{+}, Na^{+}, K^{+}, Be^{+2}, Ca^{+2}.

Table 3.7.1: Energies including ZPE corrections (Hartree), relative energies (kcal/mol), interaction energies (kcal/mol), BSSE corrected energies (Hartree), BSSE corrected relative energies (kcal/mol) and distances (Å) of structure **T4** for metals Li^{+}, Na^{+}, K^{+}, Be^{+2}, Mg^{+2}, Ca^{+2}.

Thymine	*Distance(Å)*	*E(Hartree)*	*ΔE(kcal/mol)*	*IE(kcal/mol)*	E_{BSSE}	ΔE_{BSSE}
T4a_O10a_Li	1.719	-461.4081	0.00	-53.25	-461.5242	0.00
T4b_O10a_Li	1.722	-461.3931	9.42	-51.55	-461.5083	9.97
T4b_N1_Li	1.954	-461.3852	14.37	-46.60		
T4a_N1a_Li	1.913	-461.3750	20.80	-32.45		
T4a_N1b_Li	1.913	-461.3749	20.81	-32.43		
T4a_O8_Li	1.877	-461.3548	33.43	-19.82		
T4a_O10a_Na	2.092	-616.1814	0.00	-38.62	-616.2957	0.00
T4b_O10a_Na	2.098	-616.1665	9.37	-36.96	-616.2798	9.97
T4b_N1_Na	2.314	-616.1623	12.03	-34.31		
T4a_N1_Na	2.298	-616.1525	18.19	-20.42		
T4a_O8_Na	2.253	-616.1374	27.66	-10.96		
T4a_O10a_K	2.092	-1053.8080	0.00	-27.82	-1053.9228	0.00
T4b_O10a_K	2.491	-1053.7930	9.42	-26.12	-1053.9069	9.97
T4b_N1_K	2.763	-1053.7882	12.45	-23.08		
T4a_N1_K	2.777	-1053.7810	16.93	-10.89		
T4a_O10b_Be	1.455	-468.1117	0.00	-264.05	-468.2284	0.00
T4b_O10b_Be	1.456	-468.0965	9.53	-262.23	-468.2124	10.02
T4a_O10a_Be	1.363	-468.0904	13.42	-250.63		
T4b_O10a_Be	2.491	-468.0734	24.07	-247.70		
T4b_N1_Be	1.562	-468.0676	27.70	-244.06		
T4a_0_Be	-	-468.0158	60.22	-203.83		
T4a_O8_Be	1.561	-467.9661	91.38	-172.67		
T4a_O10b_Mg	1.865	-653.5038	0.00	-149.16	-653.6185	0.00
T4b_O10b_Mg	1.868	-653.4884	9.65	-147.23	-653.6024	10.08
T4b_N1_Mg	2.000	-653.4778	16.32	-140.56		
T4a_0_Mg	-	-653.4212	51.85	-97.31		
T4a_O8_Mg	2.120	-653.4121	57.55	-91.61		
T4b_0_Mg	-	-653.4077	60.32	-96.55		
T4a_O10a_Ca	2.134	-1131.0606	0.00	-97.25	-1131.1756	0.00
T4b_O10a_Ca	2.138	-1131.0432	10.92	-94.04	-1131.1574	11.46
T4b_N1_Ca	2.390	-1131.0332	17.19	-87.78		
T4a_O8_Ca	2.448	-1130.9881	45.48	-51.77		

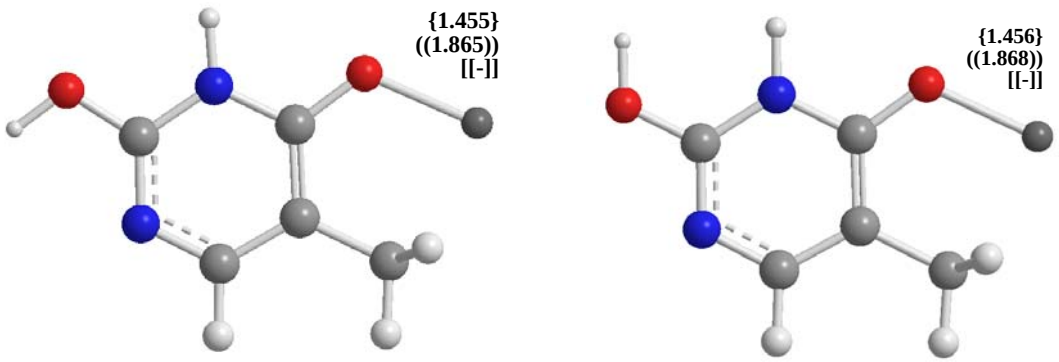

(a) **(b)**

Figure 3.7.2: Structures (a) **T4a_O10b** and (b) **T4b_O10b** with metals Be^{+2}, Mg^{+2}.

In **T4a**, alkali and alkali earth metals prefer monodentate position at M-O10. The monovalent and Ca^{+2} ions favor the same binding position, **T4a_O10a,** for global minimum structures. In Be^{+2} and Mg^{+2} complexes of **T4**, **T4a_O10b** structure is preferred due to the ability of forming six-membered ring like structure. NBO results revealed that donations from O10 to beryllium (51.88) and C4-C5 (40.32), from C11-H_a (14.58) and C11-H_b (14.57) bonds to beryllium bring an extra stability to the **T4a_O10b_Be** structure just like in **T3a_O10c_Be**. **T4a_O10b_Be** is more stable than **T4a_O10a_Be** by 13.4 kcal/mol.

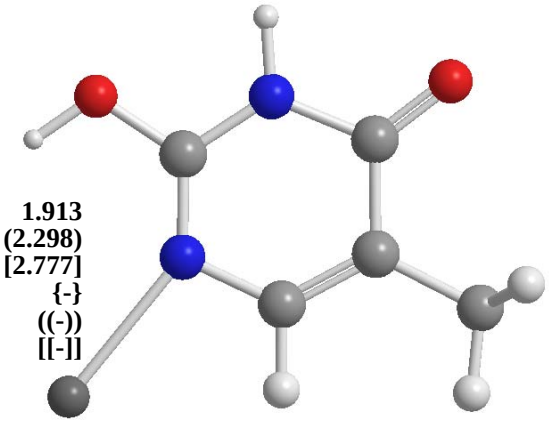

Figure 3.7.3: Structure **T4a_N1** with metals Li^+, Na^+, K^+.

Both for alkali and alkali earth metals, binding site O8 is not preferable due to the presence of hydrogen atom on that oxygen. It is found that the optimized structures of **T4a_O8** are the highest energy conformers except Mg^{+2}. It is noteworthy to state that, the interaction of K^+ cannot be modeled with **T4a_O8**. The relative energies between the lowest energy conformer and **T4a_O8** are around 30 kcal/mol for alkali metals and about 50-60 kcal/mol for alkaline earth metals. Except for the case of Na^+, metals prefer to interact with O8 nonlinearly and for the case of Ca^{+2}, bidentate binding motif is obtained where cation binds with O8 and N3.

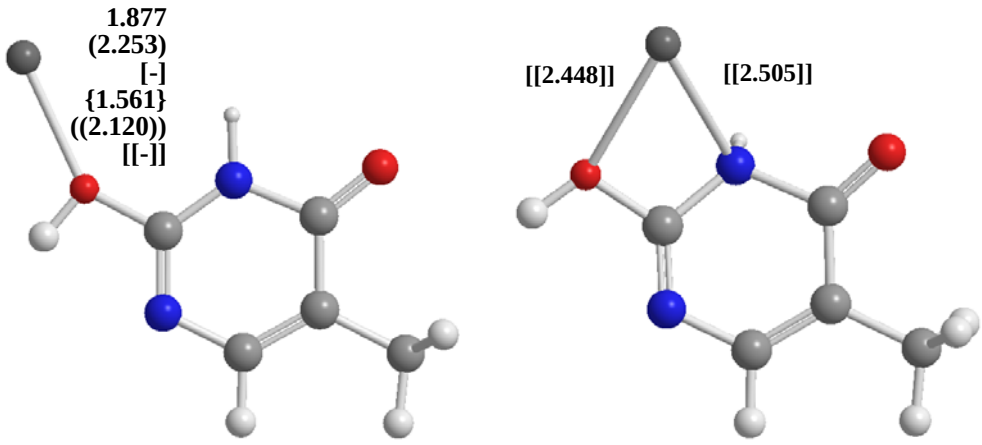

Figure 3.7.4: Structure **T4a_O8** with metals (a) Li^{+}, Na^{+}, Be^{+2}, Mg^{+2} (b) Ca^{+2}.

For **T4b**, both monodentate and bidentate binding motifs can be modeled (Figure 3.7.1-3.7.2 and Figure 3.7.5). Likewise in the case of **T4a**, cations favor the same binding site O10, independently the type of ion in the global minimum for **T4b**. Binding in the form of **T4b_O10a** is more favorable than **T4b_O10b** for alkali metals and Ca^{+2}.

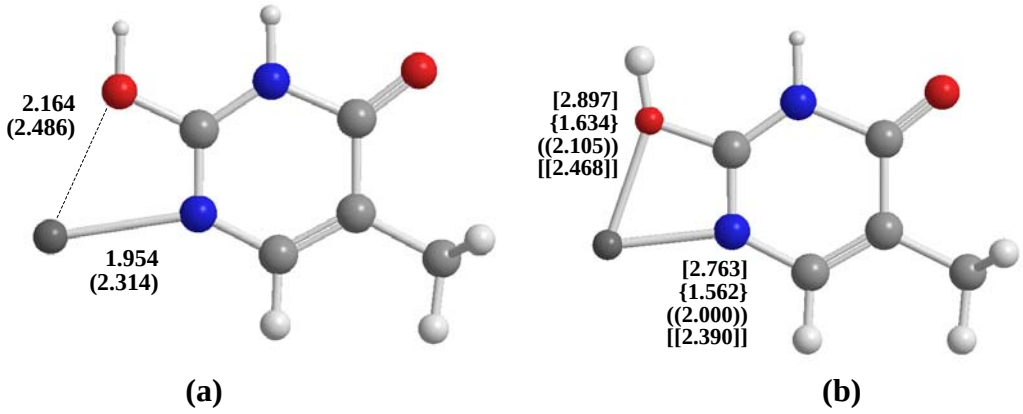

Figure 3.7.5: Structure **T4b_N1** with metals (a) Li^{+}, Na^{+} (b) K^{+}, Be^{+2}, Mg^{+2}, Ca^{+2}.

The Li^{+} and Na^{+} metals bound from nitrogen N1 to form T4b_N1 structure where the divalent atoms and K^{+} bound bidentately from O8 and N1 (Figure 3.7.5).

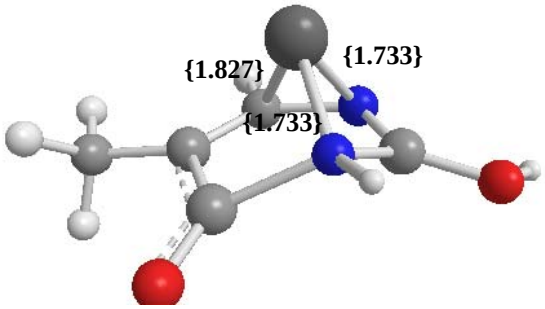

Figure 3.7.6: Structure **T4a_0** with metal Be^{+2}

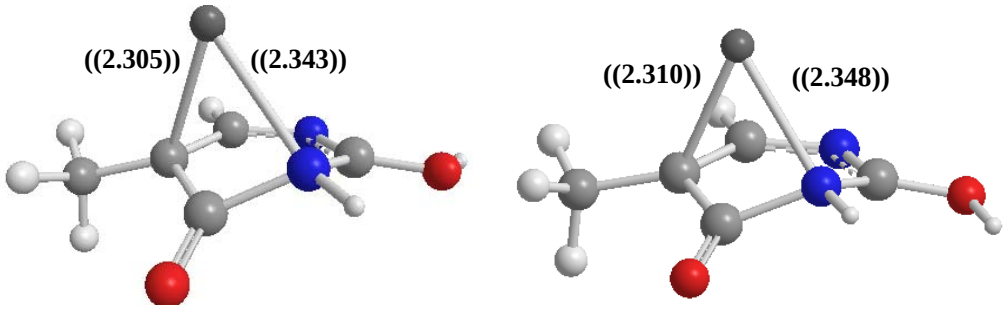

Figure 3.7.7: Structures **T4a_0** and **T4b_0** with metal Mg^{+2}.

More than one cation-π complexes can be modeled for **T4** with Be^{+2} and Mg^{+2} ions. **T4a_0_Mg** is more stable than **T4b_0_Mg** by 8.5 kcal/mol. The planarity is distorted from its original position in cation- π complexes. Binding from C6 and N3 is preferred by Be^{+2} in **T4a**. C5-C4-N3-C2 dihedral is distorted from planarity by -49.3° and -48.4° for **T4a_0_Mg** and **T4b_0_Mg** respectively.

3.8 T5

Molecule **T5** is the only dienol tautomer of **T1,** in which, 10 cation-heteroatom and 4 cation-π complexes are modeled (Figure 1.2). Four main conformers, **T5a**, **T5b**, **T5c** and **T5d** of molecule **T5**, are exist according to the position of the hydrogen atoms on O8 and O10 (Figure 3.8.1-3.8.5).

For all metals, **T5c_O8a** is the lowest energy conformer in which metals are bound to thymine from O8 in bidentate binding motif (Figure 3.8.1-3.8.2). Although there are other conformers which are bidentately bound to the thymine, in **T5c** the long range interactions between N3 and hydrogens on O8 and O10 (distances are around 2.400 Á and 2.300 Á) are the cause of extra stability.

Table 3.8.1: Energies including ZPE corrections (Hartree), relative energies (kcal/mol), interaction energies (kcal/mol), BSSE corrected energies (Hartree), BSSE corrected relative energies (kcal/mol) and distances (Å) of structure **T5** for metals Li^{+}, Na^{+}, K^{+}, Be^{+2}, Mg^{+2}, Ca^{+2}.

Thymine	*Distance(Å)*	*E(Hartree)*	*ΔE(kcal/mol)*	*IE(kcal/mol)*	E_{BSSE}	ΔE_{BSSE}
T5c_O8a_Li	2.019	-461.4034	0.00	-53.86	-461.5188	0.00
T5b_O8b_Li	2.029	-461.3975	3.72	-54.84	-461.5125	3.95
T5d_O8a_Li	2.003	-461.3968	4.14	-54.43		
T5b_O10a_Li	2.102	-461.3951	5.25	-53.32		
T5a_O8b_Li	1.929	-461.3951	5.25	-53.31		
T5d_O10a_Li	1.958	-461.3827	13.02	-45.54		
T5a_O10b_Li	1.850	-461.3687	21.78	-36.78		
T5c_O10b_Li	1.855	-461.3651	24.05	-34.51		
T5c_O8a_Na	2.359	-616.1794	0.00	-45.56	-616.2932	0.00
T5b_O8b_Na	2.388	-616.1744	3.12	-42.44	-616.2879	3.37
T5d_O8a_Na	2.340	-616.1726	4.22	-41.34		
T5b_O10a_Na	2.496	-616.1723	4.44	-41.12		
T5d_N1_Na	2.370	-616.1720	4.61	-40.95		
T5a_O8b_Na	2.268	-616.1713	5.08	-40.49		
T5d_O10a_Na	2.300	-616.1590	12.79	-32.77		
T5a_N1_Na	2.303	-616.1532	16.42	-29.14		
T5a_O10b_Na	2.227	-616.1471	20.24	-25.33		
T5c_O10b_Na	2.234	-616.1435	22.53	-23.04		
T5c_O8a_K	2.761	-1053.8041	0.00	-33.60	-1053.9187	0.00
T5b_O8b_K	2.828	-1053.7998	2.70	-30.89	-1053.9141	2.89
T5b_O10a_K	3.097	-1053.7981	3.78	-29.82		
T5d_O8a_K	2.741	-1053.7974	4.19	-29.41		
T5a_O8b_K	2.665	-1053.7967	4.65	-28.95		
T5d_O10a_K	2.710	-1053.7843	12.42	-21.18		
T5a_O10b_K	2.684	-1053.7771	16.91	-16.69		
T5c_O10b_K	2.694	-1053.7735	19.20	-14.40		
T5c_O8a_Be	1.591	-468.1011	0.00	-265.59	-468.2162	0.00
T5d_O8a_Be	1.587	-468.0954	3.52	-262.07	-468.2107	3.48
T5b_O8b_Be	1.580	-468.0919	5.72	-259.87		
T5b_O10a_Be	1.583	-468.0892	7.45	-258.15		
T5a_O8b_Be	1.558	-468.0827	11.53	-254.06		
T5d_O10a_Be	1.560	-468.0711	18.81	-246.78		
T5a_O10b_Be	1.502	-468.0311	43.90	-221.69		
T5c_O10b_Be	1.504	-468.0261	47.05	-218.55		
T5a_0_Be	-	-468.0152	53.89	-211.70		
T5c_0_Be	-	-468.0131	55.21	-210.38		
T5b_0_Be	-	-468.0058	59.80	-205.79		
T5d_0_Be	-	-468.0056	59.90	-205.69		
T5c_O8a_Mg	2.039	-653.5080	0.00	-160.02	-653.6222	0.00
T5d_O8a_Mg	2.031	-653.5021	3.65	-156.37	-653.6163	3.73
T5b_O8b_Mg	2.041	-653.5018	3.87	-156.15		
T5b_O10a_Mg	2.070	-653.4985	5.95	-154.06		
T5a_O8b_Mg	1.986	-653.4888	12.04	-147.98		
T5d_O10a_Mg	2.008	-653.4761	19.97	-140.05		
T5a_O10b_Mg	1.927	-653.4373	44.35	-115.67		
T5c_O10b_Mg	1.930	-653.4321	47.58	-112.43		
T5a_0_Mg	-	-653.4198	55.35	-104.67		
T5d_0_Mg	-	-653.4114	60.58	-99.43		
T5b_0_Mg	-	-653.4108	60.96	-99.06		

T5c_O8a_Ca	2.404	-1131.0611	0.00	-105.80	-1131.1756	0.00
T5b_O8b_Ca	2.387	-1131.0573	2.34	-103.46	-1131.1715	2.57
T5d_O8a_Ca	2.375	-1131.0552	3.66	-102.14		
T5b_O10a_Ca	2.457	-1131.0528	5.20	-100.60		
T5a_O8b_Ca	2.324	-1131.0430	11.37	-94.43		
T5d_O10a_Ca	2.351	-1131.0279	20.79	-85.01		
T5a_O10b_Ca	2.306	-1130.9981	39.54	-66.26		
T5c_O10b_Ca	2.313	-1130.9927	42.89	-62.91		

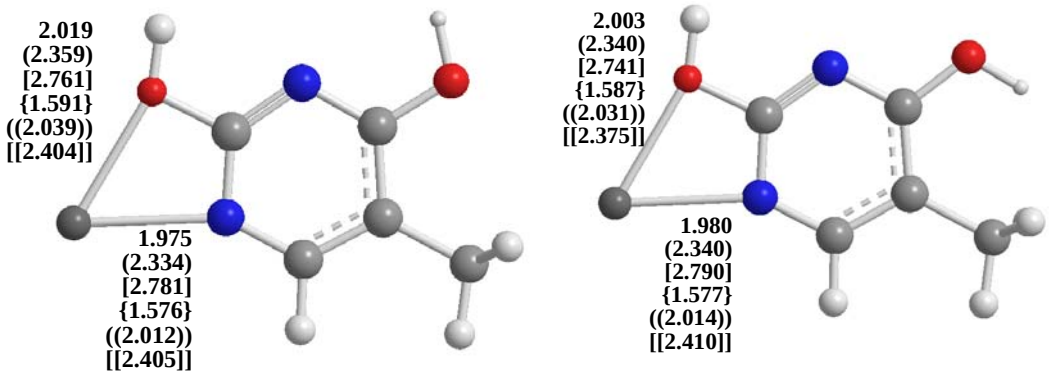

Figure 3.8.1: Structures **T5c_O8a** and **T5d_O8a**

Both for **T5b_O8b** and **T5d_O8a** conformers, the steric hindrance caused by the interaction of H atom on O10 and the methyl group on C5 increases the energy. At the same time long range interaction between H atom on O8 and N1 decreases the energy. Therefore **T5b_O8b** is observed as the second lowest energy conformer for all metals except Be^{+2} and Mg^{+2} (Table 3.8.1).

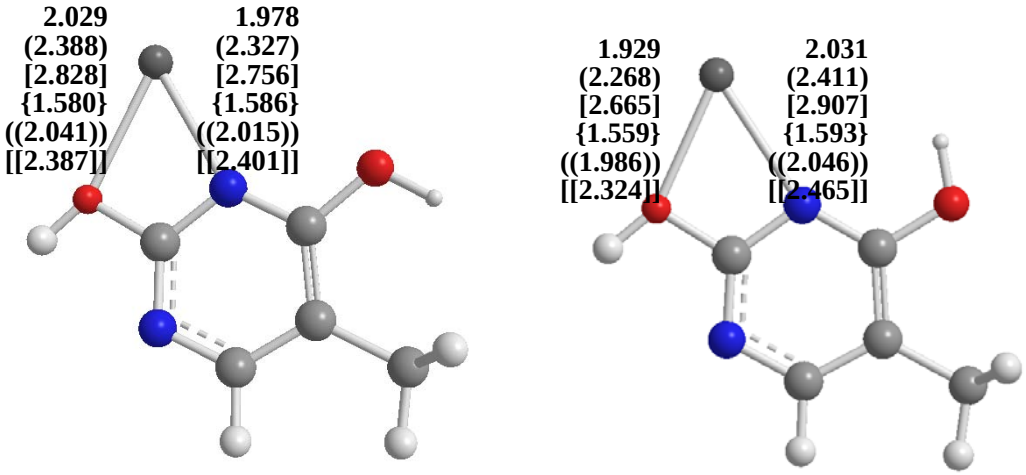

Figure 3.8.2: Structures **T5b_O8b** and **T5a_O8b**

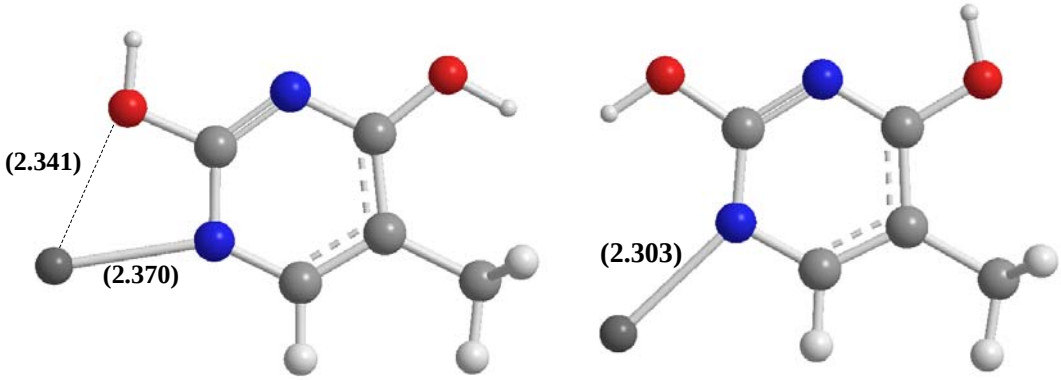

Figure 3.8.3: Structures **T5d_N1** and **T5a_N1** with Na^{+}.

Before the metalation, **T5a** conformer is the lowest energy conformer (Table 3.10.1). The presence of metal ion decreases the possibility of long range interaction between N1- H atom on O8 and N3-H atom on O10 which decreases the stability of molecule (Figure 3.8.2, Figure 3.8.3 and Figure 3.8.5).

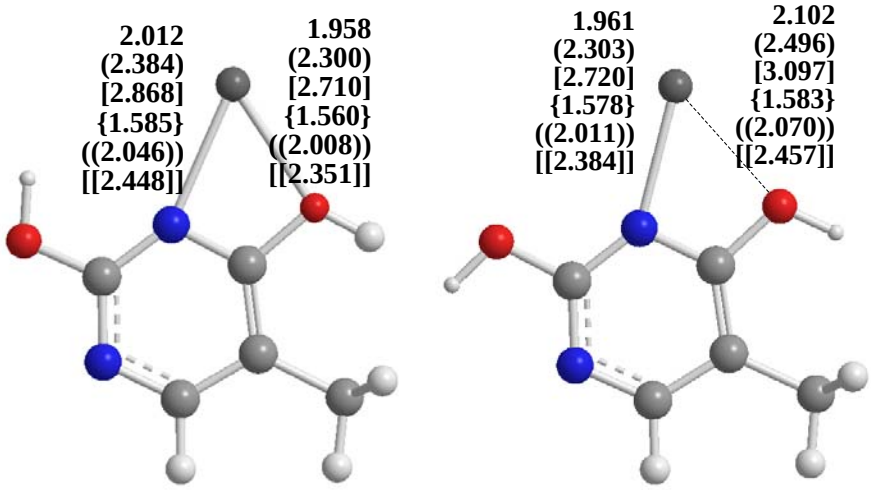

Figure 3.8.4: Structures **T5d_O10a** and **T5b_O10a**.

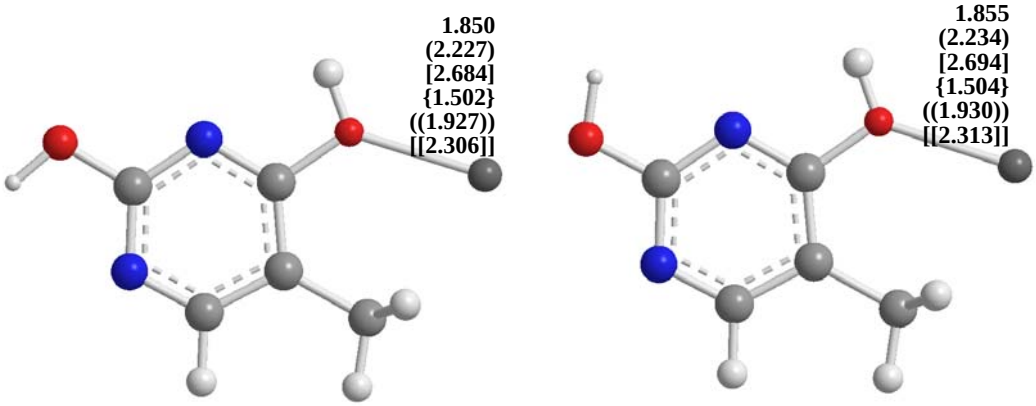

Figure 3.8.5: Structures **T5a_O10b** and **T5c_O10b.**

Comparing all **T5a_O10b** and **T5c_O10b** structures, **T5a_O10b** is lower in energy. Only Be^{+2} and Mg^{+2} ions are capable of forming cation-π complexes with the **T5**, in which, the structure is distorted from its original position and allowing cation-π complexes with nitrogens (N1 and N3) of the base.

3.9 Interactions of Transition Metals with Thymine Tautomers

Transition or d-block metals have the d-orbitals partially filled and thus they can be qualified as free radicals. Transition metals interact with more than two different sites and their interactions with DNA are more complicated. They usually bind

Table 3.9.1: Energies including ZPE corrections (Hartree), relative energies (kcal/mol), interaction energies (kcal/mol) and distances (Å) of all thymine tautomers for metals Cu^{+},Cu^{+2}, Fe^{+2}.

Thymine	*Distance(Å)*	*E(Hartree)*	*ΔE(kcal/mol)*	*IE(kcal/mol)*
T1_O10b_Cu	1.871	-2094.1706	0.00	-61.43
T1_0_Cu	2.045	-2094.1362	21.61	-39.82
T1_O10a_Cu^{+2}	1.929	-2093.7108	0.00	-252.61
T1_O10b_Fe	1.856	-1716.8995	0.00	-205.39
T1_0_Fe	-	-1716.8569	26.73	-178.66
T2a_O8a_Cu	1.883	-2094.1726	0.00	-75.26
T2a_O8b_Cu	2.140	-2094.1713	0.83	-74.43
T2a_0_Cu	2.040	-2094.1172	34.76	-40.50
T2a_O10b_Cu	1.978	-2094.1168	34.98	-40.28
T2a_O8a_Cu^{+2}	1.910	-2093.7107	0.00	-265.16
T2a_O8b_Cu^{+2}	2.466	-2093.6995	7.09	-258.07
T2a_0_Fe	-	-1716.8517	46.07	-187.98
T2a_O10b_Fe	1.990	-1716.8506	46.78	-194.63
T2a_O10c_Fe	1.959	-1716.8375	54.99	-179.06
T3a_O10a_Cu	1.885	-2094.1691	0.00	-78.95
T3a_0_Cu	2.052	-2094.1122	35.72	-43.23
T3a_O10a_Cu^{+2}	1.899	-2093.7051	0.00	-267.46
T3a_0_Cu^{+2}	2.131	-2093.6285	48.06	-219.39
T3b_O10c_Fe	1.839	-1716.9216	0.00	-247.65
T3a_0_Fe	-	-1716.8364	53.50	-184.23
T4a_O10b_Cu	1.871	-2094.1597	0.00	-65.29
T4a_0_Cu	2.057	-2094.1283	19.70	-45.59
T4a_O10a_Cu^{+2}	1.922	-2093.7021	0.00	-257.88
T4b_O10c_Fe	1.890	-1716.8783	0.00	-210.56
T4a_0_Fe	-	-1716.8472	19.52	-183.31
T5c_N1_Cu	1.916	-2094.1663	0.00	-73.02
T5a_0_Cu	2.062	-2094.1201	28.99	-42.89
T5c_N1_Cu^{+2}	1.968	-2093.6978	0.00	-258.74
T5a_0_Fe	-	-1716.8510	0.00	-188.10
T5a_O10b_Fe	1.969	-1716.8352	9.89	-178.21

directly to the bases and indirectly to the phosphate groups. Most of the transition metals react chemically with the N7 atom of purine or N3 of pyrimidine and perturb the double helix [28].

Among the elements present in plants, animals and bacteria, copper is one of the most abundant transition metals [46]. Although both Cu^{+} and Cu^{+2} complexes play an important role in chemistry and in biochemistry, studies of the interactions of the divalent cation with biological systems are limited to very few cases [19,47,48-51]. The interaction of Cu^{+} with some amino acids has been studied by mass spectrometry, [52] to our knowledge; no experimental information about the Cu^{+} affinity for nucleic acid bases is available.

3.9.1 Interaction of Copper(I) with Thymine

Copper(I) ion forms a number of stable complexes with thymine tautomers in which it appears most frequently mono-coordinated. The stability order is the following: **T2-Cu^{+}>T1-Cu^{+}>T3-Cu^{+}>T5-Cu^{+}>T4-Cu^{+}** (Figure 3.9.1).

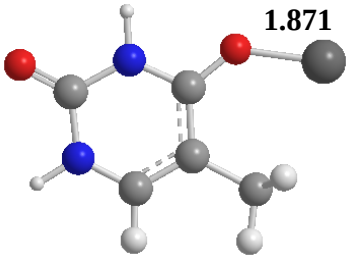

T1_O10b_Cu

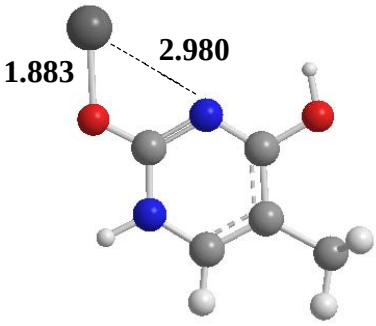

T2a_O8a_Cu

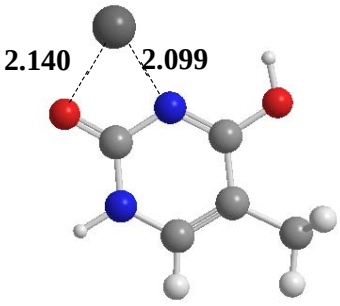

T2a_O8b_Cu

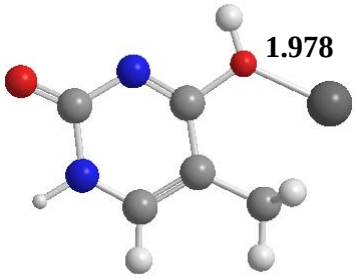

T2a_O10b_Cu

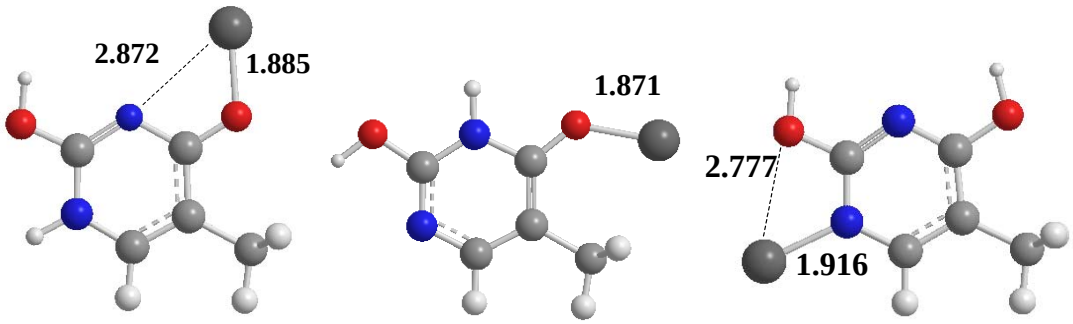

Figure 3.9.1: Structures of thymine tautomers with Cu^+.

In the thymine complexes, the cation is mostly linked to oxygen atoms. The O8–Cu^+ bond length measures 1.883Å in the most stable **T2a–Cu^+** structure. In this tautomeric form, the O10 atom appears to be a less favorable site for the Cu^+ attachment, the energy value associated with the obtained complex being higher of 34.98 kcal/mol with respect to the absolute minimum. Comparing with the interaction of nucleic bases with alkali metal ions, it is seen that copper induces a considerable decrease in the C4-O10-M valence angle (132.9° in Cu^+ versus 174.2° in Li^+, 174.9° in Na^+ and 178.3° in K^+ with **T1**). The interaction energies values of thymine and Cu^+ complexes range from -30.51 to -83.90 kcal/mol.

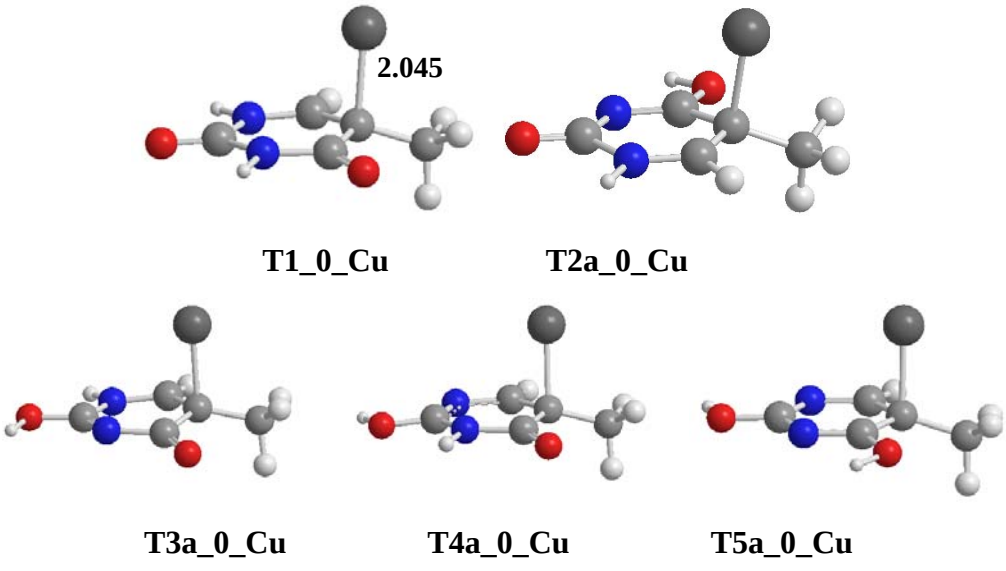

Figure 3.9.2: σ-bond interactions of thymine tautomers with Cu^+.

The cation–π interactions cannot be observed as in the cases of alkali and alkaline earth metals. The metal ion placed above the base ring but copper ion directly linked to the C5 atom after optimization. The complexes lose completely the characteristics

of cation–π complexes and Cu^{+} ions form σ-bond with C5 atom with length around 2.05 Å (Figure 3.9.2).

3.9.2 Interaction of Copper(II) with Thymine

The variety of spectroscopic techniques used until now to study DNA–Cu^{+2} complexes [48-53] generally are unable to give detailed structural information, especially when the metal ion is present at low concentrations. All the adducts obtained by the interaction of the tautomers of thymine with Cu^{+2} ion show a similar energetic trend as seen in the interaction of the same tautomers with the Cu^{+}. The five tautomeric forms of free thymine give rise to five complexes with the Cu^{+2} cation The stability order is the following: **T1-Cu^{+2}>T2-Cu^{+2}>T3-Cu^{+2}>T4-Cu^{+2} >T5-Cu^{+2}** (Figure 3.9.3)**.** The copper ion is always mono-coordinated to oxygen or nitrogen atoms except for the case in the **T2a_O8b_Cu^{+2}** structure (Figure 3.9.3). In the most stable **T1_O10a_Cu^{+2}** structure, the O8–Cu^{+2} bond length measures 1.929Å which is 0.076 Å longer than the corresponding bond for the Cu^{+} complex with **T1** (Figure 3.9.1 and Figure 3.9.3). Energies of the **T**-Cu^{+} complexes are lower than **T**-Cu^{+2} of same tautomers by 285-300 kcal/mol.

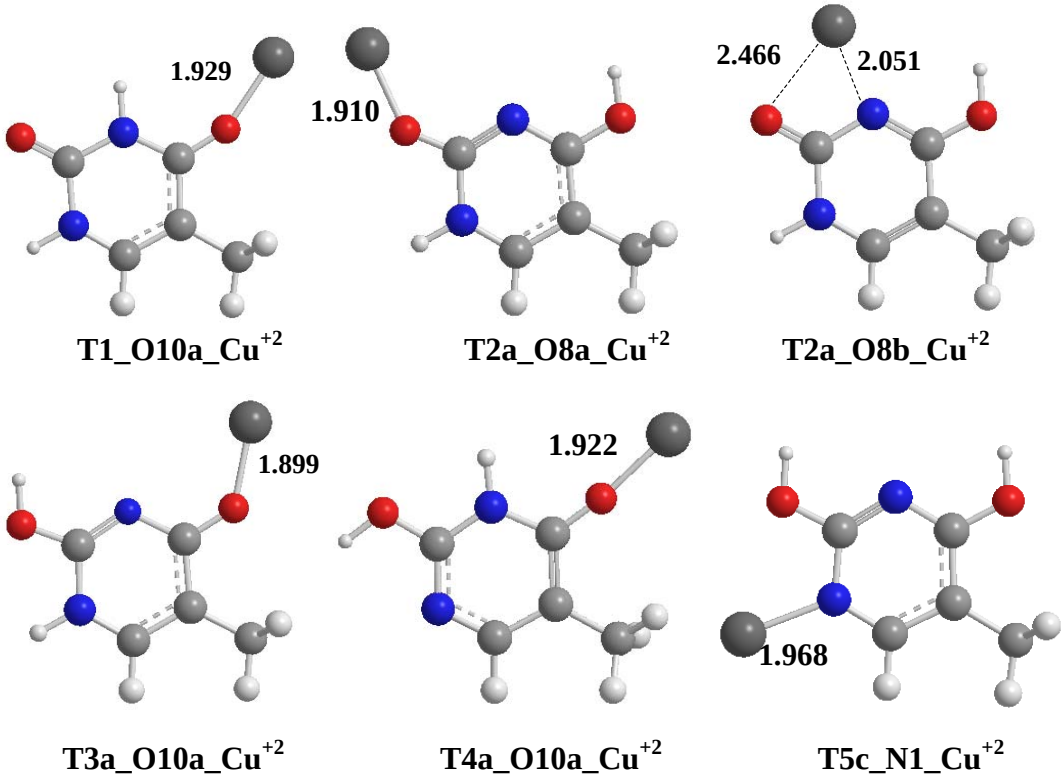

Figure 3.9.3: Structures of thymine tautomers with Cu^{+2}.

The interaction energies values of thymine and Cu^{+2} complexes range from -220.12 kcal/mol to -267.52 kcal/mol. The divalent cation has a better affinity for RNA and DNA bases. The reason for this behavior is certainly the different chemistry of a closed-shell as opposed to an open-shell system. As in the case of T-Cu^{+}, no cation–π complex can be modeled but σ-bond interaction is modeled between C5 of T3 and Cu^{+2} with length 2.131 Å (Figure 3.9.4).

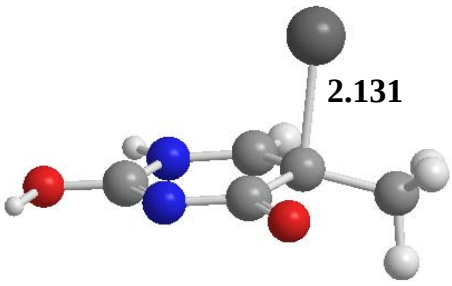

T3a_0_Cu^{+2}

Figure 3.9.4: σ-bond interaction of **T3** with Cu^{+2}.

3.9.3 Interaction of Iron(II) with Thymine

Iron(II) ion forms a number of stable complexes with nucleic acid base tautomers. The five tautomeric forms of free thymine give rise to five complexes with the Fe^{+2} cation. The stability order is the following: **T2-Fe^{+2}>T3-Fe^{+2}>T1-Fe^{+2}>T4-Fe^{+2}> T5-Fe^{+2}** (Figure 3.9.5). In the complexes thymine, Fe^{+2} is mostly linked to oxygen atoms (O8 and O10). In the most stable **T2b**-Fe^{+2} structure, cation form bidentate binding motif with O8 and N3 atoms. In the lowest energy conformer of **T3** and **T4** complexes with Fe^{+2}, cation binds to O10 and C5 out of the ring plane and the ring planarity is slightly distorted. Five-membered ring like structure formation can be seen when Fe^{+2} interact with O10 and C11 of the thymine tautomers. But those planar structures are generally the highest energy conformers.

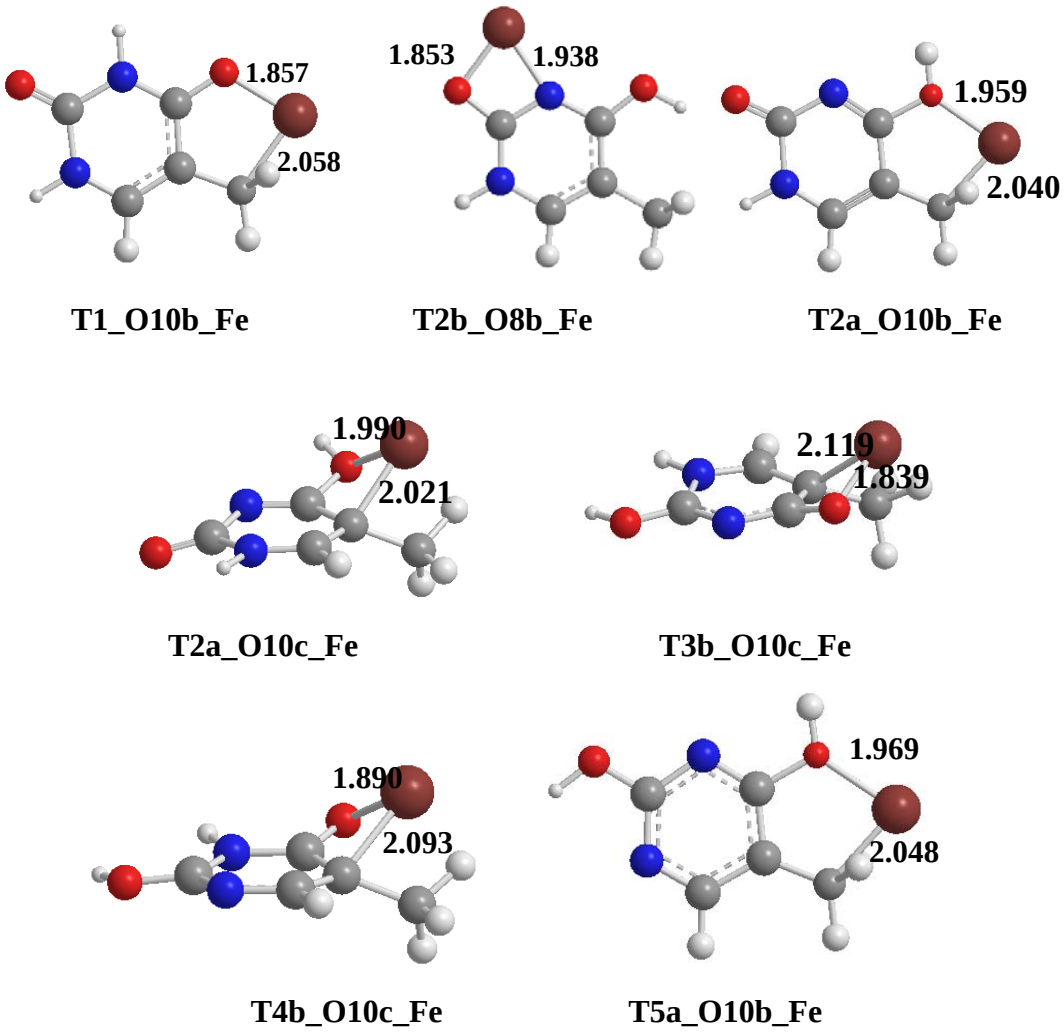

Figure 3.9.5: Structures of thymine tautomers with Fe^{+2}.

Fe^{+2} ions are capable of forming cation-π complexes with the thymine tautomers. As in the cases of alkali and alkaline earth metal, the structures are distorted from its original position and allowing cation-π complexes with the atoms of the base (Figure 3.9.6). It is noteworthy to state that, N1-C2-N3-C4 dihedral is distorted from planarity by -67.4°, -61.8°, -61.4°, -49.7°, -36.5° for **T1_0_Fe, T2a_0_Fe, T3a_0_Fe, T4a_0_Fe** and **T5a_0_Fe** respectively. (Figure 3.9.6). The energy differences between absolute minimum of **T-Fe** structures and cation-π complexes of thymine and iron are in the range of 20 kcal/mol to 55 kcal/mol. The interaction energies values of thymine and Fe^{+2} complexes range from -178.21 to -247.65 kcal/mol (Table 3.10.1).

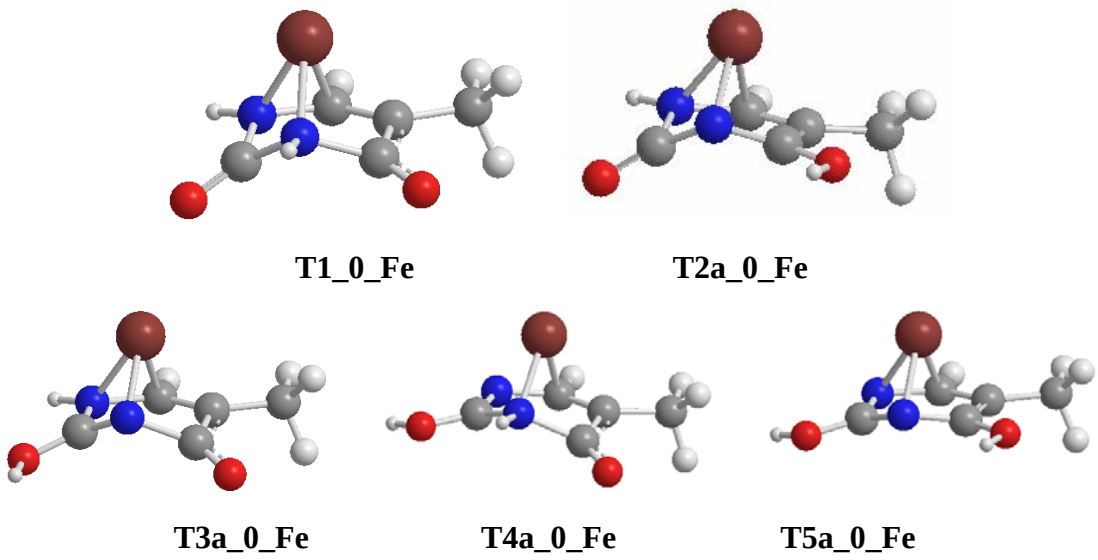

Figure 3.9.6: Cation-π structures of thymine tautomers with Fe^{+2}.

Since no experimental studies are available on Cu–DNA or –RNA base complexes, comparison of the results obtained by the B3LYP/6–31++G** computational scheme with experimental data is not possible; however, previous investigations, performed on alkali and alkaline earth metal ion–nucleic base complexes, have proved that the level of theory used provides reliable equilibrium geometries and energetics, so data arising from this study can be used with confidence.

3.10 Comparison of Thymine Tautomers

The interpretation of absorption spectroscopy experimental data usually reveals different tautomeric forms because they have considerably different spectra. While in some cases, it is difficult to detect the rare tautomers when a single form dominates. It has been pointed out that spectroscopic methods are incapable of detecting less than 0.1-1.0% of a minor tautomer [54]. Thus, the theoretical prediction of various physicochemical properties of different tautomeric forms is essential for understanding the behavior of thymine itself and can be a useful guide for studying its other derivatives. The thymine molecule may exist in various tautomeric forms differing from each other by the position of the protons, which may be bound to either ring nitrogen atoms or oxygen atoms. The five possible keto-enol tautomers and three methylated tautomers were examined and their geometries were fully optimized in this work (Figure 1.3). The relative energies of the tautomers are shown

in Table 3.10.1. The presences of these tautomers are confirmed by harmonic vibrational frequency calculations.

Table 3.11.1: Electronic energies including ZPE corrections for thymine tautomers

Conformer	*E*	*ΔE*
T1	-454.055755	0.00
T4a	-454.038663	10.73
T2a	-454.035708	12.58
T5a	-454.034832	13.13
T5c	-454.033016	14.27
T4b	-454.026363	18.44
T3a	-454.026360	18.45
T5b	-454.025605	18.92
T5d	-454.025519	18.97
T2b	-454.023984	19.94
T3b	-454.010546	28.37
T1_Me	-493.339533	0.00
T2a_Me	-493.320375	12.02
T3a_Me	-493.309221	19.02
T2b_Me	-493.308884	19.23
T3b_Me	-493.292824	29.31

Molecule **T1** has the lowest energy among the thymine tautomers as expected. The stability order of the thymine tautomers is found to be: **T1**>**T4**>**T2**>**T5**>**T3**. The stability order of the stable methyl tautomers **T1_Me**, **T2_Me**, **T3_Me** are same as the main tautomers **T1**, **T2**, **T3**, in other words, substitution of thymine base at N1 position by CH_3 did not change the order of the stability. The results are in accordance with previous experimental [55] and theoretical results found with AM1 [56].

Among the conformers of the tautomers (a-b), the lower energy conformers are the ones where the hydrogen of the hydroxyl group has a long range interaction with the nitrogen atom (**T2a**, **T3a**, **T4a**, **T5a**). The distance between hydrogen on O8 or O10 with nitrogen located nearby is about 2.300 Å. The structures are stabilized by 7-8 kcal/mol due to this long range interaction. Energy of the conformer **T2a** is lower than the conformer **T3a** by 6 kcal/mol, due to the delocalization ability of charge on **T2a** structure.

Other than **T1**, the rest of the tautomers have a capability of bidentate metal binding. This can change the stability order of tautomers in case of metal binding since the bidentate bound structures are more stable than monodentate bound structures.

3.11 Effect of Metal Binding on Tautomer Structures and Their Relative Stabilities

It is well established by experiments that metalation of nucleobases can cause shifts of nucleobase hydrogens, such as protonation, deprotonation, and formation of rare tautomers of bases.

The order of stability of metalated tautomers are: **T1**>**T2**>**T3**>**T4**>**T5** for alkali metals Li^{+}, Na^{+}, K^{+}, **T3**>**T2**>**T1**>**T4**>**T5** for Be^{+2} and **T2**>**T3**>**T1**>**T5**>**T4** for Mg^{+2} and Ca^{+2}. In the case of transition metals, the stability orders are: **T2>T1>T3>T5>T4** for Cu^{+}, **T1>T2>T3>T4>T5** for Cu^{+2} and **T2>T3>T1>T4>T5** for Fe^{+2}. It is seen that metalation is remarkably influence relative stabilities. For the

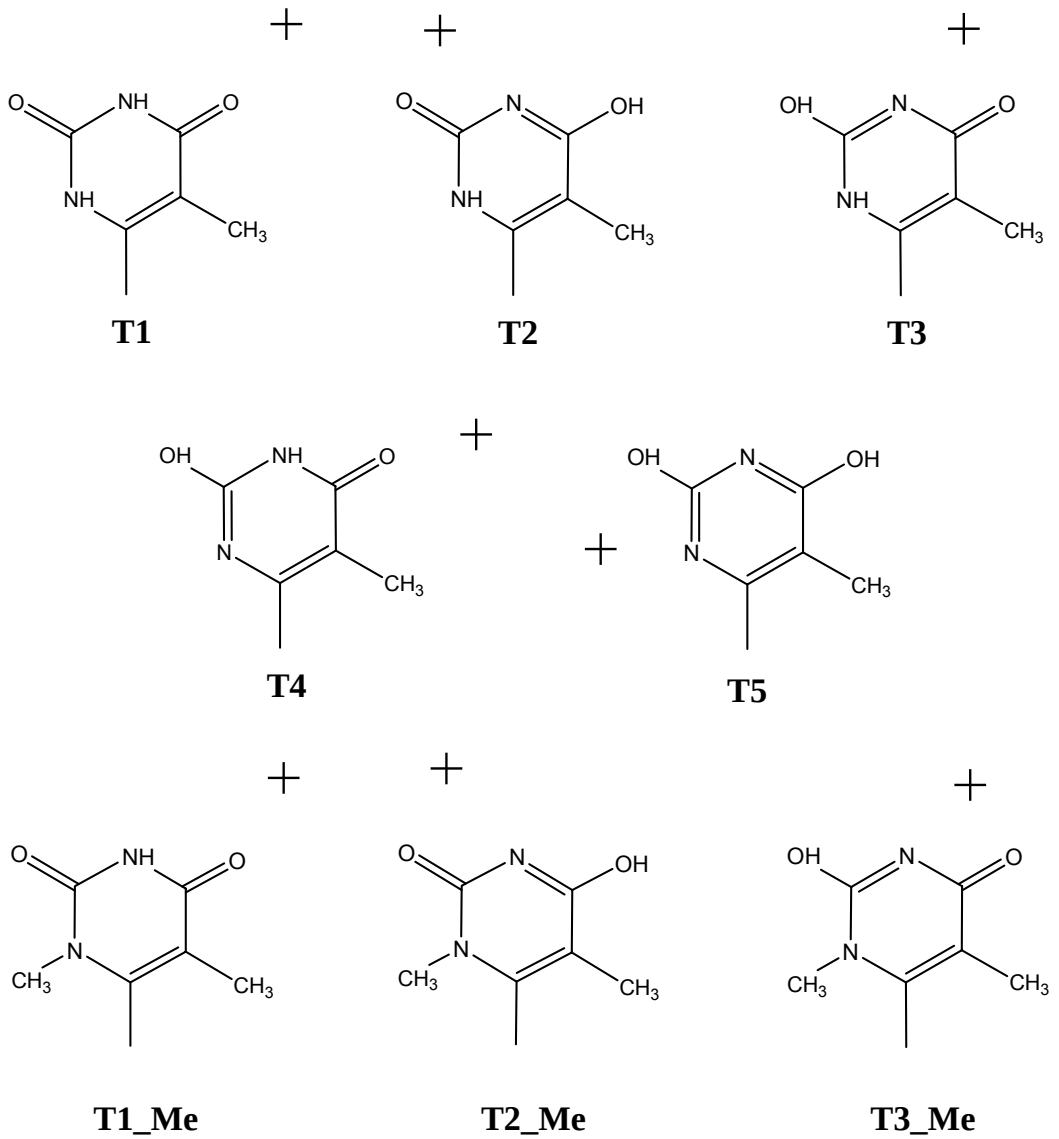

Figure 3.11.1: Lowest energy cation-heteroatom structures.

methylated thymine tautomers, stability order of metal complexes is in accordance with the non-methylated tautomers, which is: **T1_Me**>**T2_Me**>**T3_Me** for alkali metals and **T2_Me**>**T3_Me**>**T1_Me** for alkaline earth metals.

It is found that, the same binding motif is preferred for the lowest energy structures independently from the type of metal ions. The preferred conformation may differ for the different type of cations. Metal ions favor O10 binding site in monodentate manner in **T1**. In the case of **T1- Be** binding, six-membered ring interaction can be seen because of the long range interaction between C11 and Be^{+2}. In **T2**, O8 is the preferred site for all metals. Metals prefer to bind in bidentate manner. For **T3**, all metals preferred O10 binding site. Cations bind bidentately to O10 interacting with N3. For the cases of Be^{+2} and Mg^{+2}, six-membered ring interaction is observed. Li^{+}, Na^{+}, K^{+} and Ca^{+2} form monodentate binding with O10 in **T4**, but for Be^{+2} and Mg^{+2} six-membered ring interaction is seen as in the cases of **T1** and **T3**. In **T5**, for all metals bidentate binding motif N1-M-O8 is observed. In the cases of methylated thymines metals show the same manner in accordance with the cases of non-methylated ones (Figure 3.11.1).

In total there are four cations, Li^{+}, Be^{+2}, Mg^{+2}, and Ca^{+2}, that are capable of forming cation-π complexes with thymine tautomers, of which Be^{+2} can form cation-π complexes with all tautomers. No cation-π structure can be optimized with Na^{+} and K^{+}. For **T1**, cation-π complexes are optimized with Li^{+}, Be^{+2}, Mg^{+2}, and Ca^{+2}. For **T2**, cation-π complexes are optimized with Be^{+2}, Mg^{+2}, and Ca^{+2}. For **T3**, only cation-π complex is optimized with Be^{+2}. For **T4** and **T5**, cation-π complexes are optimized with Be^{+2} and Mg^{+2}. The optimized structures show a distortion of the nucleobase planar ring structures and the degree of distortion varied among the different complexes.

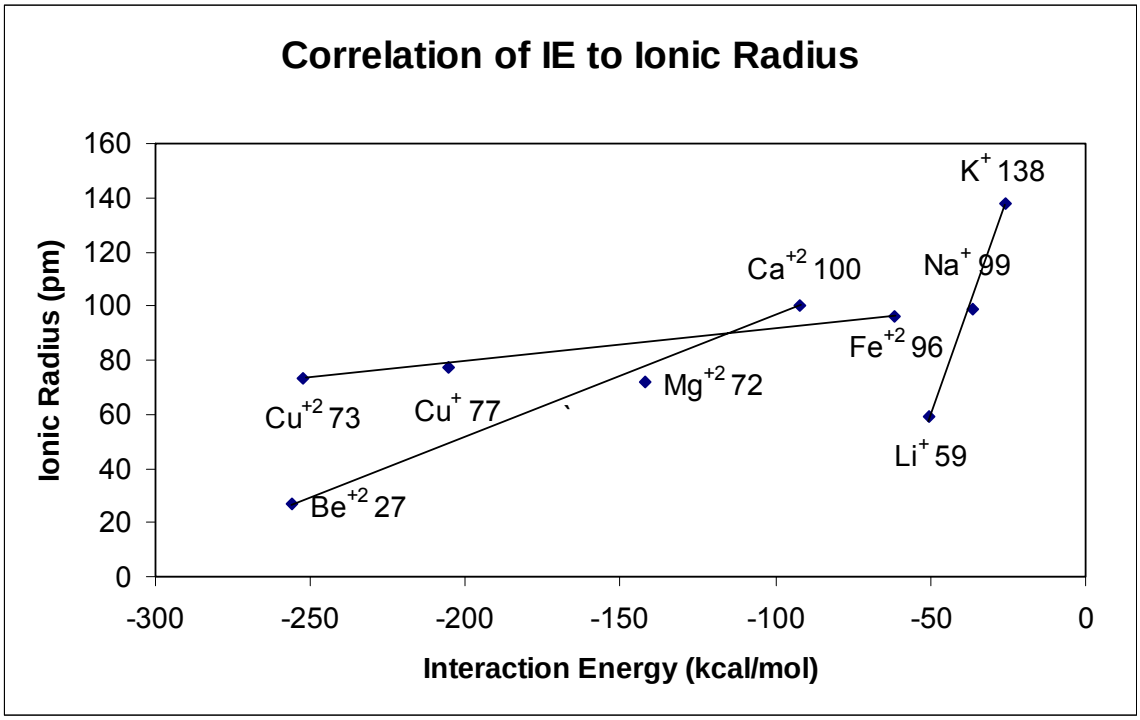

Figure 3.11.2: Correlation of interaction energies for **T1** to ionic radius [57].

The interaction energy of metal ions to T1 tautomers correlates well with the ionic radius of the metal. The interaction energies for the metal ions become smaller as the size of the cations decrease. Same correlation is seen for **T2**, **T3, T4** and **T5.**

4. CONCLUSION

The metal binding capability of thymine and its tautomers with metal ions have been investigated at B3LYP/6-31++G** level. The comparisons with the available experimental data and previous theoretical results have been performed. The interaction energies have a qualitative agreement with the experimental data. [4,22].

The interaction pattern might change in thymine tautomers relative to the type of the metal ion. It is found that both cation-π and cation-heteroatom binding are possible between metal ions and thymine tautomers. In addition to that binding motifs, binding between copper(I and II) ions and carbon atom C5 of the base ring is modeled. In cation-π structures, distortion of the planar ring structure of thymine takes place. In the cation-heteroatom interactions in which a cation directly binds to the heteroatom(s) of the thymine and is usually located in the same plane as ring atoms. The cations can interact mostly in a bidentate manner with thymine and its tautomers which were found to be stronger than monodentate binding. In the formation of a six-membered ring like structure an extra stability is brought by an interaction of a metal ion with ring atoms.

The interaction energies of thymine tautomers decrease with increasing atomic number for the same group elements. The order of stability doesn't affected by methylation from N1 site. Metalation significantly affects stability order of tautomer.

It is seen that, the BSSE corrected relative energies (ΔE_{BSSE}) with respect to global minimum are in accordance with the energies without BSSE corrections (ΔE).

It can be concluded that the result of this study will provide useful information about the thymine-metal interactions which can be used for further studies dealing with processes in biological systems.

REFERENCES

[1] **Miescher**, **F.,** 1897. *Die histochemischen und physiologischen arbeiten*, Vogel, Leipzig.

[2] **Levene, P.**, 1919.*J. Biol. Chem.*, **40**, 415 – 424.

[3] **Watson, J.D and Crick, F.H.C.,** 1953. *Nature,* 171-737.

[4] (a) **Cerda, B. A. and Wesdemiotis, C.**, 1996. *J. Am. Chem. Soc*., **118**, 11884. (b) **Cerda, B. A. and Wesdemiotis, C.**, 1995. *J. Am. Chem. Soc*., **117**, 9734.

[5] **Poater, J., Sodupe, M., Bertran, J. and Sola, M.**, 2005. *Molecular Physics*, **103**, 163-173.

[6] **Topal, M.D. and Fresco, J.R**., 1979. *Nature,* **263,** 285.

[7] (a) **Eichhorn, G. L.** Advances in *Inorganic Biochemistry: Vol. 3, Metal Ions in Genetic Information Transfer*, 1981Marzilli, L. G., Eds. Elsevier/North-Holland: New York,. (b) **Sigel, H., Sigel, A.,** *Metal Ions in Biological Systems: Vol. 25, Interrelations Among Metal Ions, Enzymes, and Gene Expression*, 1989. *Eds. Marcel Dekker,* New York. (c) **Sigel, A., Sigel, H.,** *Metal Ions in Biological Systems: Vol. 33, Probing of Nucleic Acids by Metal Ion Complexes of Small Molecules*, 1996.*Eds. Marcel Dekker,* New York. (d) **Nakano, S. I., Fujimoto, M., Hara, H., Sugimoto**, 1999. *N. Nucleic Acids Res*. ***27***, 2957.

[8] **Villafranca, J. J. and Nowak, T**., 1992. *In The Enzymes, Vol. 20*, Sigman, D. S., Ed. Academic Press: New York, p 63.

[9] **Cowan, J. A., 1993.** *Inorganic Biochemistry. An Introduction*, VCH Publishers: New York.

[10] **Saenger, W**., 1983. Principles of Nucleic Acid Structure, Springer-Verlag, New York.

[11] **Sigel, A. and Sigel, H.**, 1996. Interactions of Metal Ions with Nucleotides, *Nucleic Acids and Their Constituents. Metal Ions in Biological Systems: Vol. 32, Eds. Marcel Dekker,* New York.

[12] **E. Hammarsten,** *Biochem. Z.*, 144 (1924) 383.

[13] **Tian, S. X., Zhang, C.F., Chen X.J., Xu, Z.U**, 1999. *Chem. Phys.*, 242, 217–225.

[14] **Yang, Z. and Rodgers, M. T.**, 2005. *Int. J. Of Mass Spect.*, 241, 225-242.

[15] **Lubomir, R. and Sponer**, **J.,** 2003. *J. Phys. Chem. B.*, 107, 1913–1923.

[16] **Munoz, J., Sponer, J., Hobza, P. and Luque, F.J.**, 2001. *J. Phys.Chem.*, **105**, 6051-6060.

[17] **Lee, G.Y**, 2006. *Bull. Korean Chem. Soc.*, **27**, 3, 419–422.

[18] **Zhu, W., Luo, X., Puah, C., Tan, X., Shen, J., Gu, J., Chen, K. and Jiang, H.**, 2004. *J. Phys. Che. A*, **108**, 4008–4018.

[19] **Burda, J., Sponer, J. and Hobza, P.**, 1996. *J. Phys. Chem.*, **100**, 7250–7255.

[20] **Rodgers, M.T. and Armentrout, P.B.**, 2000. *J. Am. Chem. Soc.*, **122**, 8548-8558.

[21] **Kabelec, M. and Hobza P.**, 2006. *J. Phys. Chem. B.*, **110**, 14515-14523.

[22] **Monajjemi, M., Ghiasi, R., Passdar, H., Mollaamin, S., Ketabi, S., Chahkandi, B. and Karimkhani, M.**, 2003. *Internet Electron. J. Mol. Des.*, **2**, 741-756.

[23] **Robertazzi, A. and Platts, J. A.**, 2005. *J. Biol. İnorg. Chem.*, **10**, 854-866.

[24] **Sponer, J., Sabat, M., Burda, J., Leszczyinski, J., Hobza, P. and Lippert, B.**, 1999. *JBIC*, **4**, 537-545.

[25] **Glusker, J.P., Katz, A. and Bock, C.**,1999. *The Rigaku Journal*, **16**, 8-16.

[26] **Del Bene, J.**,1984. *E. J. Phys. Chem*., **88**, 5927.

[27] **Egli, M.**, 2002. *Chem. Biol.*, **9**, 277

[28] **Anastassopoulou, J.**, 2003. *J. Mol. Struct*., 651–653, 19–26.

[29] **Frisch, M. J., Trucks, G. W., Schlegel, H. B., Scuseria, G. E., Robb, M. A., Cheeseman, J. R., Montgomery, Jr., J. A., Vreven, T., Kudin, K. N., Burant, J. C., Millam, J. M., Iyengar, S. S., Tomasi, J., Barone, V., Mennucci, B., Cossi,M., Scalmani, G., Rega, N., Petersson, G. A., Nakatsuji, H., Hada, M., Ehara, M., Toyota, K., Fukuda, R., Hasegawa, J., Ishida, M., Nakajima, T., Honda, Y., Kitao, O., Nakai, H., Klene, M., Li, X., Knox, J. E., Hratchian, H. P., Cross, J. B., Bakken, V., Adamo, C., Jaramillo, J., Gomperts, R., Stratmann, R. E., Yazyev,O., Austin, A. J., Cammi, R., Pomelli,**

C., Ochterski, J. W., Ayala, P. Y., Morokuma, K., Voth, G. A., Salvador, P., Dannenberg, J. J., Zakrzewski, V. G., Dapprich, S., Daniels, A. D., Strain, M. C., Farkas, O., Malick, D. K., Rabuck, A. D., Raghavachari, K., Foresman, J. B., Ortiz, J. V., Cui, Q., Baboul, A. G., Clifford, S., Cioslowski, J., Stefanov, B. B., Liu, G., Liashenko, A., Piskorz, P., Komaromi, I., Martin, R. L., Fox, D. J., Keith, T., Al-Laham, M. A., Peng, C. Y., Nanayakkara, A., Challacombe, M., Gill, P. M. W., Johnson, B., Chen,W., Wong, M. W., Gonzalez, C. and Pople, J. A., 2004. *Gaussian 03*, Revision B.04, Gaussian, Inc., Wallingford, CT**.**

[30] **Grotendorst, J.,** *NIC Series Volume 25: High Performance Computing in Chemistry.*

[31] **Hobza, P. and Sponer, J.**, 1999. *Chemical Reviews,* **99**, 3247-3276.

[32] **Fermi E.**, 1927. Un Metodo statistico per la determinazione di alcune priorieta dell'atome, *Rend. Accad. Naz. Lincei,* **6**, 602

[33] **Hohenberg, P. and Kohn, W.**,1965. *Phys. Rev.,* **140**, A1133

[34] **Kohn, W. and Sham, L.J.**, 1965. *Phys. Rev.,* **140**, A1133

[35] **Becke, A. D.**, 1993. *J. Chem. Phys*., **98**, 5648.

[36] (a) **Becke, A. D.**, 1998. *Phys. ReV. A*, **38**, 3098. (b) **Lee, C., Yang, W. and Parr, R. G.**, 1988. *Phys. ReV. B*, **37**, 785. (c) **Vosko, S. H., Wilk, L. and Nusair, M.**, 1980. *Can. J. Phys*., **58**, 1200.

[37] **Hoyau, S. and Ohanessian, G.**, 1997. *Chem. Phys. Lett.*, **280**, 266.

[38] **Kemper, P.R., Weis, P., Bowers, M.T. and Maitre, P.**, 1998. *J. Am. Chem. Soc.*, **120**, 13494.

[39] **Alcamı, M., Luna, A., Mo, O., Yanez, M., Boutreau, L. and Tortajada, J.**, 2002. *J. Phys. Chem. A*, **106**, 2641.

[40] **Gonzalez, L., Mo, O. and Yanez, M.**, 1997. *J. Comput. Chem.*, **18**, 1124.

[41] **Gonzalez, L., Mo, O. and Yanez, M.**, 1998. *J. Chem. Phys*., **109**, 139.

[42] **Gonzalez, L., Mo, O. and Yanez M.**, 1997. *J. Phys. Chem. A*, **101**, 9710.

[43] **Andzelm, J. and Wimmer, E.** 1992 *J. Chem. Phys***., 96,** 1280.

[44] **Mercero, J. M., Matxain, J. M., Lopez, X., York, D. M., Largo, A., Eriksson, L. A. and Ugalde, J. M.,** 2005**,** *Int. J. Mass Spectrom***., 240,** 37.

[45] **Frisch, M.J., Del Bene, J.E., Binkley, J.S. and Schaefer, H.F., III**., 1986. *J. Chem. Phys*., **84,** 2279.

[46] **Theil, E.C. and Raymond, K.N,**. 1994, In Bioinorganic Chemistry, Eds. Bertini I, *Gray HB, Lippard, S.J., Selverstone Valentine, J.,* University Science Books, Sausalito, CA.

[47] **Meggers, E., Holland, P.L.,Tolman, W.B., Romesberg, F.E. and Schultz, P.G.** 2000. *J. Am. Chem. Soc*., **122**, 10714.

[48] **Deng, H. and Kebarle, P.,** 1998. *J. Am. Chem. Soc*., **120**, 2925.

[49] **Marino, T., Russo, N. and Toscano, M.,** 2000. *J. Inorg. Biochem*., **79**,179.

[50] **Marino, T., Russo, N. and Toscano, M.**, 2001. *Inorg. Chem*., **40**, 6439.

[51] **Stangret, J. and Savoie, R.,** 1993. *J. Mol. Struct*., **297**, 91.

[52] **Cerda, B.A. and Wesdemiotis, C.,** 1999. *Int. J. Mass Spectrom*.**, 107**, 185–187.

[53] **Theophanides, T. and Anastassopoulou, J.,** 2002. *Crit. Rev. Oncol./Hematol*., **42**, 57 .

[54] **Shugar, D. and Szczepaniak K.**,1981. *Int. J. Quantum Chem.*, **20**, 573.

[55] **Person, W.B., Szczepaniak, K., Szczesniak, M., Kwiatkowski, J.S., Hernandez, L. and Czerminski, R.**, 1989. *J. Mol. Struct. (Theochem)*, **194**, 239.

[56] **Katritzky, A.R. and Karelson, M.M.**, 1991. *J. Am. Chem. Soc.*, **113**, 1561.

[57] **Petrucci, R.H., Harwood, W.S. and Herring F.G.,** 2002. General Chemistry: Principles and Modern Applications**,** 8th ed**.,** Prentice Hall**,** Upper Saddle River, NJ.

APPENDIX

Gaussian Input File

```
%mem=240mw
%nproc=4
%chk= T1_Li
# opt freq=noraman b3lyp/6-31++g(d,p) pop=(nbo,savenbo) geom=connectivity
density=current

T1-Li optimization with nbo calculations

1 1
 N
 C                  1             B1
 H                  2             B2    1             A1
 C                  2             B3    1             A2    3             D1
 C                  4             B4    2             A3    1             D2
 H                  5             B5    4             A4    2             D3
 H                  5             B6    4             A5    2             D4
 H                  5             B7    4             A6    2             D5
 C                  4             B8    2             A7    1             D6
 O                  9             B9    4             A8    2             D7
 N                  9            B10    4             A9    2             D8
 C                 11            B11    9            A10    4             D9
 O                 12            B12   11            A11    9            D10
 H                 11            B13    9            A12    4            D11
 H                  1            B14    2            A13    4            D12
 Li                 1            B15    2            A14    4            D13

   B1            1.38141287
   B2            1.08493343
   B3            1.35395795
   B4            1.50152403
   B5            1.09504504
   B6            1.09505648
   B7            1.09367019
   B8            1.46852186
   B9            1.22469878
   B10           1.40703411
   B11           1.38473736
   B12           1.22147944
   B13           1.01399842
   B14           1.01024407
   B15           1.56434576
   A1          115.01296497
   A2          122.72538839
   A3          123.90498440
   A4          110.85247351
   A5          110.85107684
   A6          111.08421185
   A7          117.94996946
   A8          125.05114254
   A9          114.84008653
   A10         127.91330935
   A11         124.06729400
   A12         116.31427750
   A13         121.05483905
   A14          70.77390917
   D1          179.98563454
   D2         -179.98933696
   D3          120.89341670
   D4         -120.90404303
```

```
  D5             -0.00776181
  D6              0.00754606
  D7           -179.98976997
  D8              0.00749324
  D9             -0.00895998
  D10          -180.00000000
  D11          -179.98788146
  D12          -179.94248002
  D13            43.54526135

1 2 1.5 12 1.0 15 1.0
2 3 1.0 4 2.0
3
4 5 1.0 9 1.0
5 6 1.0 7 1.0 8 1.0
6
7
8
9 10 2.0 11 1.0
10
11 12 1.0 14 1.0
12 13 2.0
13
14
15
16
```

BIOGRAPHY

I was born in İstanbul in 1982. I completed my high school education in İstanbul (Özel Coşkun Lisesi) in 2000. I have received my B.Sc degree from Bilkent University, Mathematics Department in 2004. I am still a graduate student of Istanbul Technical University, Computational Science and Engineering Department. My research area is Molecular Modeling and Scientific Computing.